

Supporting Information for:

Iron(II) Complexes of a Hemilabile SNS Amido Ligand: Synthesis, Characterization and Reactivity

Uttam K. Das,[†] Stephanie L. Daifuku,[‡] Theresa E. Iannuzzi,[‡] Serge I. Gorelsky,[†] Ilia Korobkov,[†] Bulat Gabidullin,[†] Michael L. Neidig,^{*‡} and R. Tom Baker^{*†}

[†] Department of Chemistry and Biomolecular Sciences and Centre for Catalysis Research and Innovation, University of Ottawa, Ottawa, ON K1N 6N5, Canada

[‡] Department of Chemistry, University of Rochester, Rochester, NY 14627, USA

Table of Contents

NMR, UV/Vis, EI-MS and IR spectra

Figure S1. ^1H NMR spectrum of 2-(2-methylthiobenzylidene) methylthioaniline	S3
Figure S2. $^{13}\text{C}\{\text{H}\}$ NMR spectrum of 2-(2-methylthiobenzylidene) methylthioaniline	S4
Figure S3. ^1H NMR spectrum of $[\text{S}^{Me}\text{N}^H\text{S}^{Me}]$ ligand	S5
Figure S4. $^{13}\text{C}\{\text{H}\}$ NMR spectrum of $[\text{S}^{Me}\text{N}^H\text{S}^{Me}]$ ligand	S6
Figure S5. UV-vis spectrum of $[\text{S}^{Me}\text{N}^H\text{S}^{Me}]$ ligand	S7
Figure S6. High-Resolution EI-MS spectrum of $[\text{S}^{Me}\text{N}^H\text{S}^{Me}]$ ligand	S8
Figure S7. IR (ATR) spectrum of $[\text{S}^{Me}\text{N}^H\text{S}^{Me}]$ ligand	S9
Figure S8. ^1H NMR spectrum of $[\text{Fe}(\kappa^3\text{-S}^{Me}\text{NS}^{Me})_2]$ (1)	S10
Figure S9. UV-vis spectrum of $[\text{Fe}(\kappa^3\text{-S}^{Me}\text{NS}^{Me})_2]$ (1)	S11
Figure S10. Cyclic voltammogram of $[\text{Fe}(\kappa^3\text{-S}^{Me}\text{NS}^{Me})_2]$ (1)	S12
Figure S11. ^1H NMR spectrum of $[\text{Fe}(\kappa^3\text{-S}^{Me}\text{NS}^{Me})_2(\text{bpy})]$ (3)	S13
Figure S12. ^1H NMR spectrum of $[\text{Fe}(\kappa^2\text{-S}^{Me}\text{NS}^{Me})_2(\text{CNxylyl})_2]$ (4)	S14
Figure S13. $^{13}\text{C}\{\text{H}\}$ NMR of $[\text{Fe}(\kappa^2\text{-S}^{Me}\text{NS}^{Me})_2(\text{CNxylyl})_2]$ (4)	S15
Figure S14. IR (ATR) spectrum of $[\text{Fe}(\kappa^2\text{-S}^{Me}\text{NS}^{Me})_2(\text{CNxylyl})_2]$ (4)	S16
Figure S15. ^1H NMR spectrum of $[\text{Fe}(\kappa^3\text{-S}^{Me}\text{NS}^{Me})_2(\text{dmpe})]$ (5)	S17
Figure S16. $^{31}\text{P}\{\text{H}\}$ NMR spectrum of $[\text{Fe}(\kappa^3\text{-S}^{Me}\text{NS}^{Me})_2(\text{dmpe})]$ (5)	S18
Figure S17. ^1H NMR spectrum of $[\text{Fe}(\kappa^3\text{-S}^{Me}\text{NS}^{Me})(\kappa^3\text{-S}^{Me}\text{N}^H\text{S}^{Me})](\text{NTf}_2)$ (6)	S19
Figure S18. ^{19}F NMR spectrum of $[\text{Fe}(\kappa^3\text{-S}^{Me}\text{NS}^{Me})(\kappa^3\text{-S}^{Me}\text{N}^H\text{S}^{Me})](\text{NTf}_2)$ (6)	S20
Figure S19. ^1H NMR spectrum of $[\text{Fe}(\kappa^2\text{-S}^{Me}\text{NS}^{Me})(\kappa^3\text{-triphos})]$ (7)	S21
Figure S20. $^{31}\text{P}\{\text{H}\}$ NMR spectrum of $[\text{Fe}(\kappa^2\text{-S}^{Me}\text{NS}^{Me})(\kappa^3\text{-triphos})]$ (7)	S22
Figure S21. ^{19}F NMR spectrum of $[\text{Fe}(\kappa^2\text{-S}^{Me}\text{NS}^{Me})(\kappa^3\text{-triphos})]$ (7)	S23
Figure S22. ^{11}B and $^{11}\text{B}\{\text{H}\}$ NMR spectra of dehydrogenation catalysis of AB with 7	S24
Figure S23. $^{31}\text{P}\{\text{H}\}$ NMR spectra of dehydrogenation catalysis of AB with 7	S25
Figure S24. ^1H NMR spectrum of dehydrogenation catalysis of AB with 7	S26
Figure S25. ^{11}B and $^{11}\text{B}\{\text{H}\}$ NMR spectra of dehydrogenation catalysis of DMAB with 7	S27

Figure S26. $^{31}\text{P}\{\text{H}\}$ NMR spectrum of dehydrogenation catalysis of DMAB with 7	S28
Figure S27. ^1H NMR spectrum of dehydrogenation catalysis of DMAB with 7	S29
X-ray Crystallography	
Experimental	S30
Table S1: X-ray diffraction data collection and refinement parameters	S31
Mössbauer and Magnetic Circular Dichroism (MCD) Spectroscopy	
Experimental	S32
Figure S28. 80 K Mössbauer spectrum of a frozen solution of ^{57}Fe -enriched (1)	S33
Figure S29. 80 K Mössbauer spectrum of $[\text{Fe}(\kappa^2\text{-S}^{Me}\text{NS}^{Me})(\kappa^3\text{-triphos})](\text{NTf}_2)$ (7)	S33
Computational studies	
Experimental	S34
Computational parameters	S35
References	S46

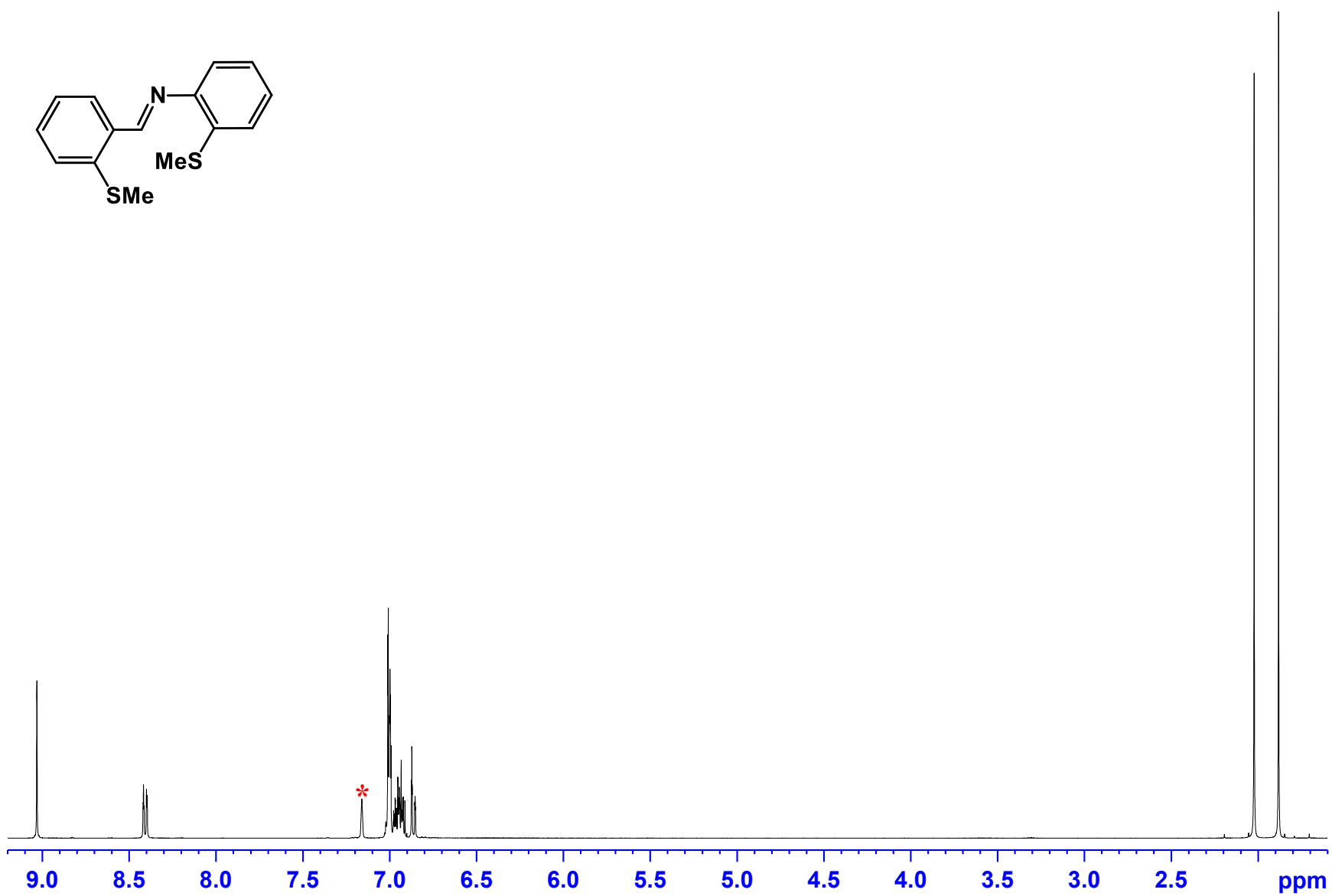


Figure S1. ^1H NMR (300 MHz, C_6D_6) spectrum of 2-(2-methylthiobenzylidene) methylthioaniline.

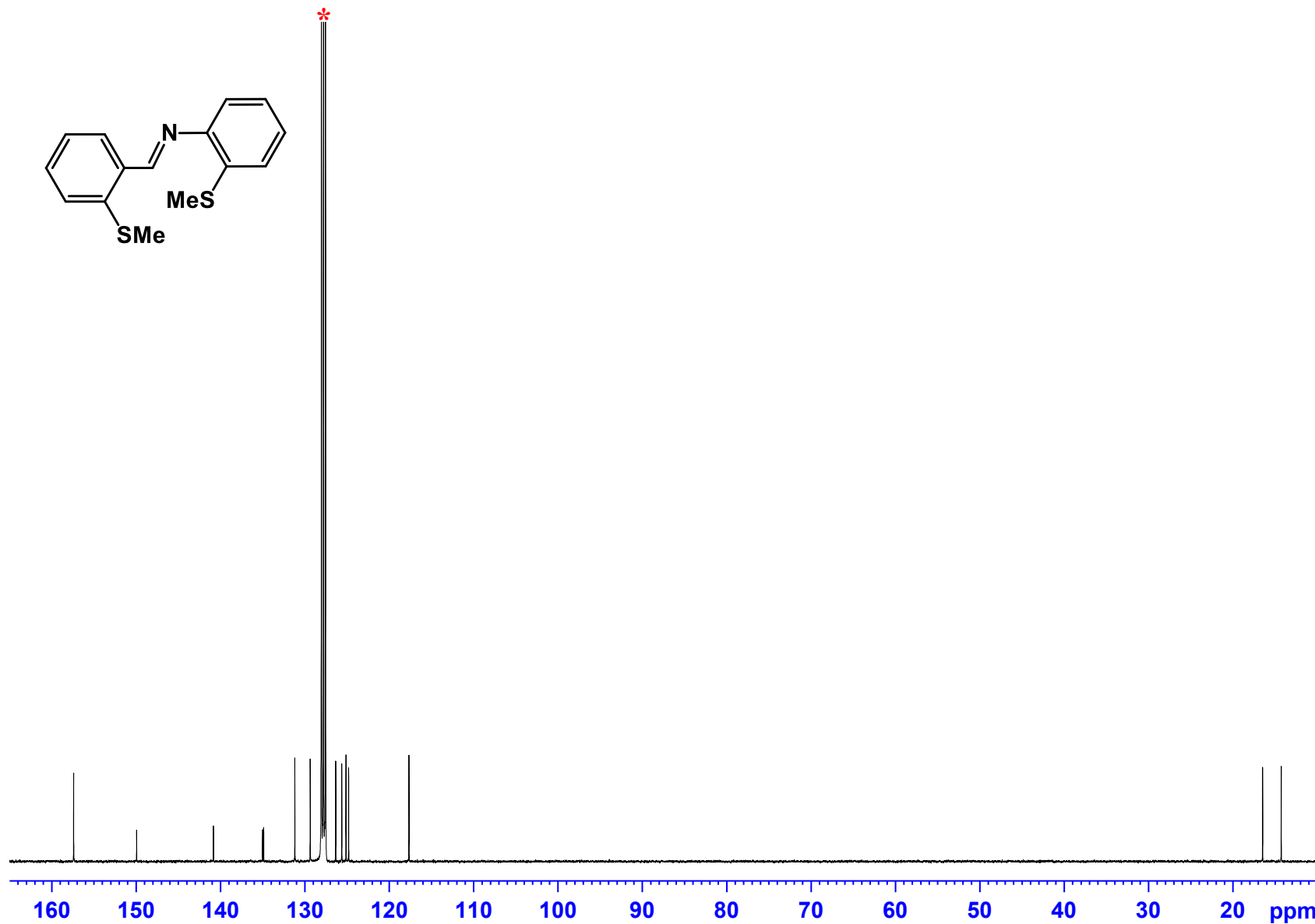


Figure S2. $^{13}\text{C}\{\text{H}\}$ NMR (100 MHz, C_6D_6) spectrum of 2-(2-methylthiobenzylidene) methylthioaniline.

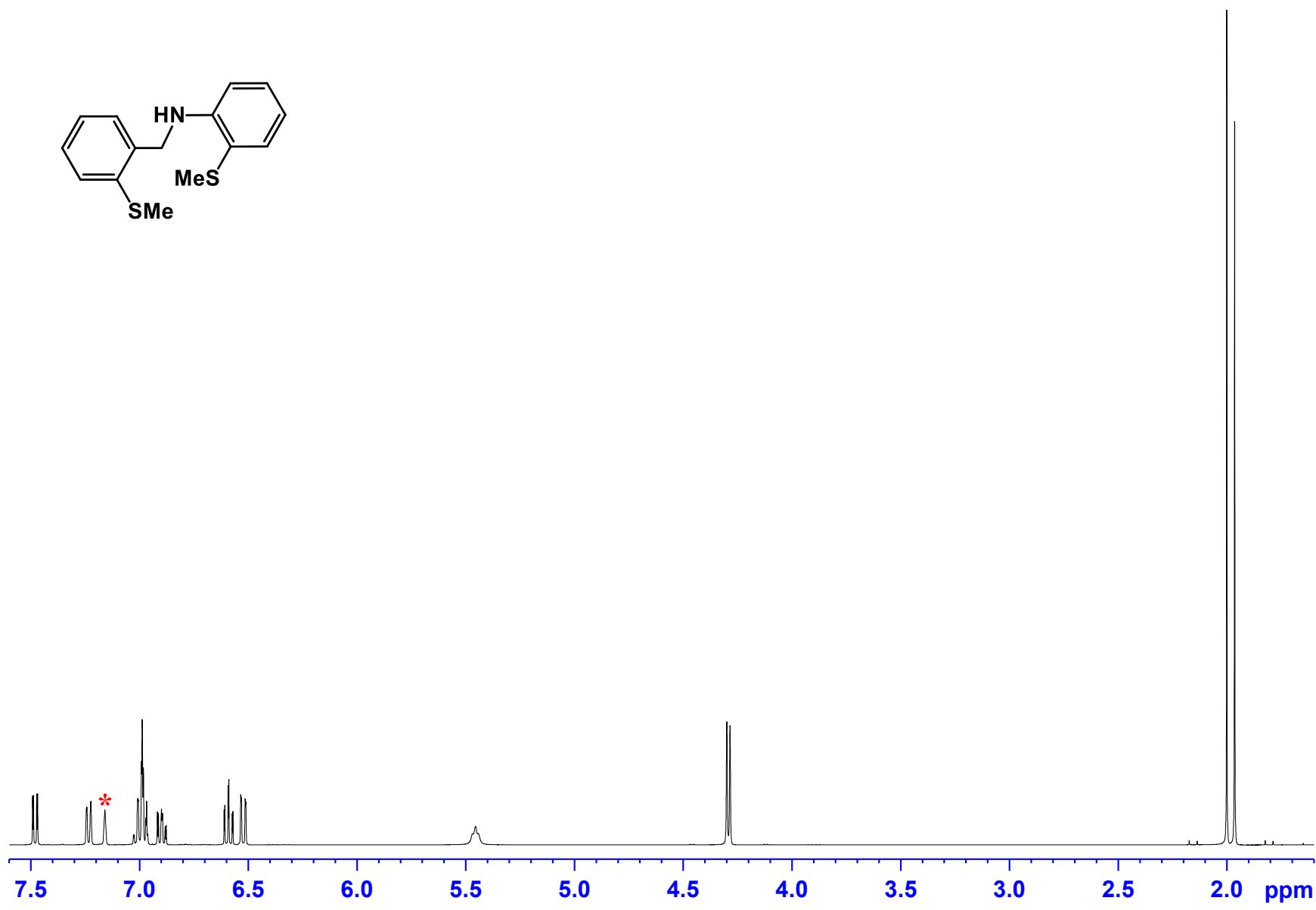


Figure S3. ^1H NMR (300 MHz, C_6D_6) spectrum of $[\text{S}^{Me}\text{N}^H\text{S}^{Me}]$ ligand.

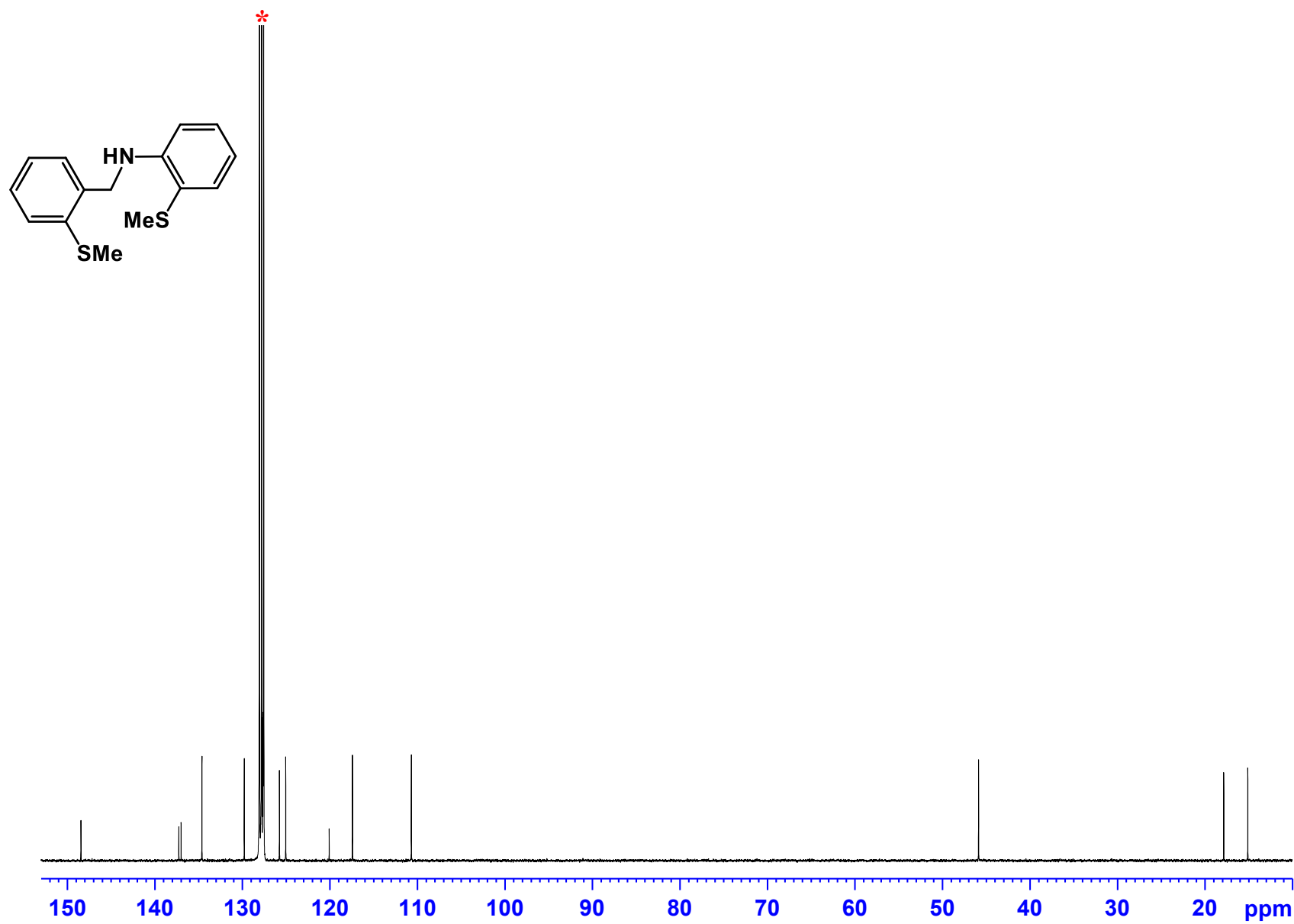


Figure S4. $^{13}\text{C}\{^1\text{H}\}$ NMR (100 MHz, C_6D_6) spectrum of $[\text{S}^{\text{Me}}\text{N}^{\text{H}}\text{S}^{\text{Me}}]$ ligand.

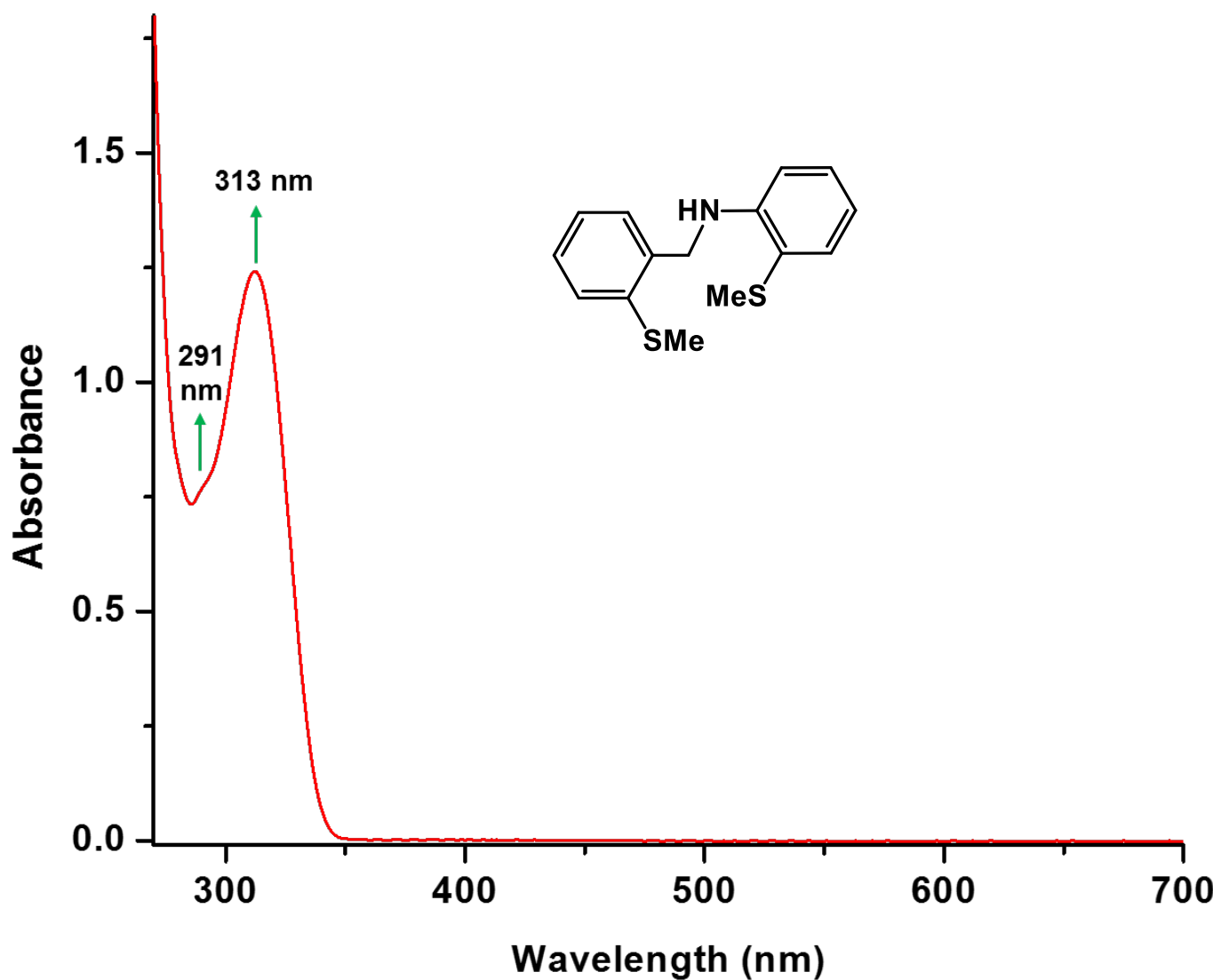


Figure S5. UV-vis spectrum of $[S^{Me}N^H S^{Me}]$ ligand (1.8×10^{-4} M in THF).

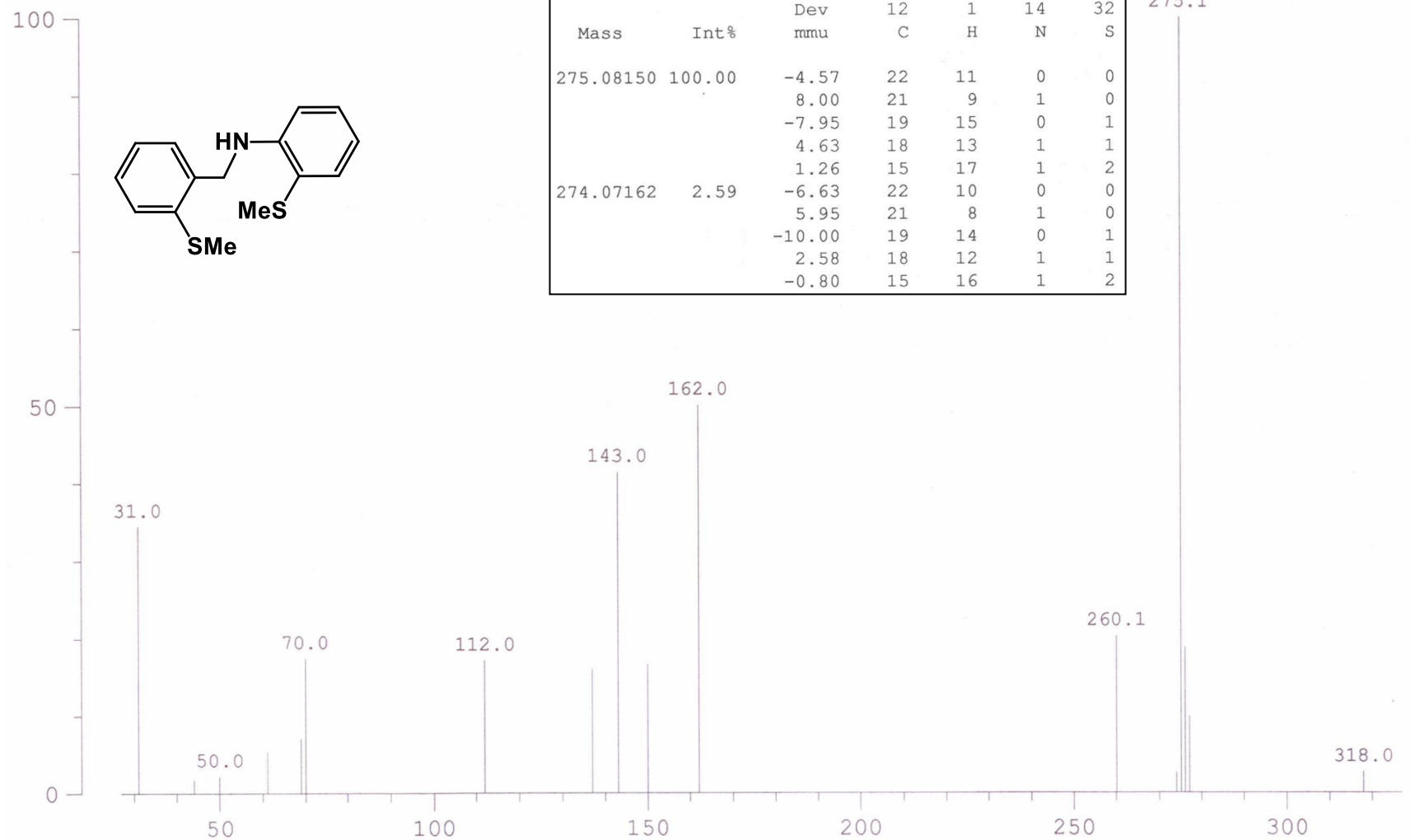


Figure S6. High-Resolution EI-MS spectrum of $[S^{Me}N^HS^{Me}]$ ligand.

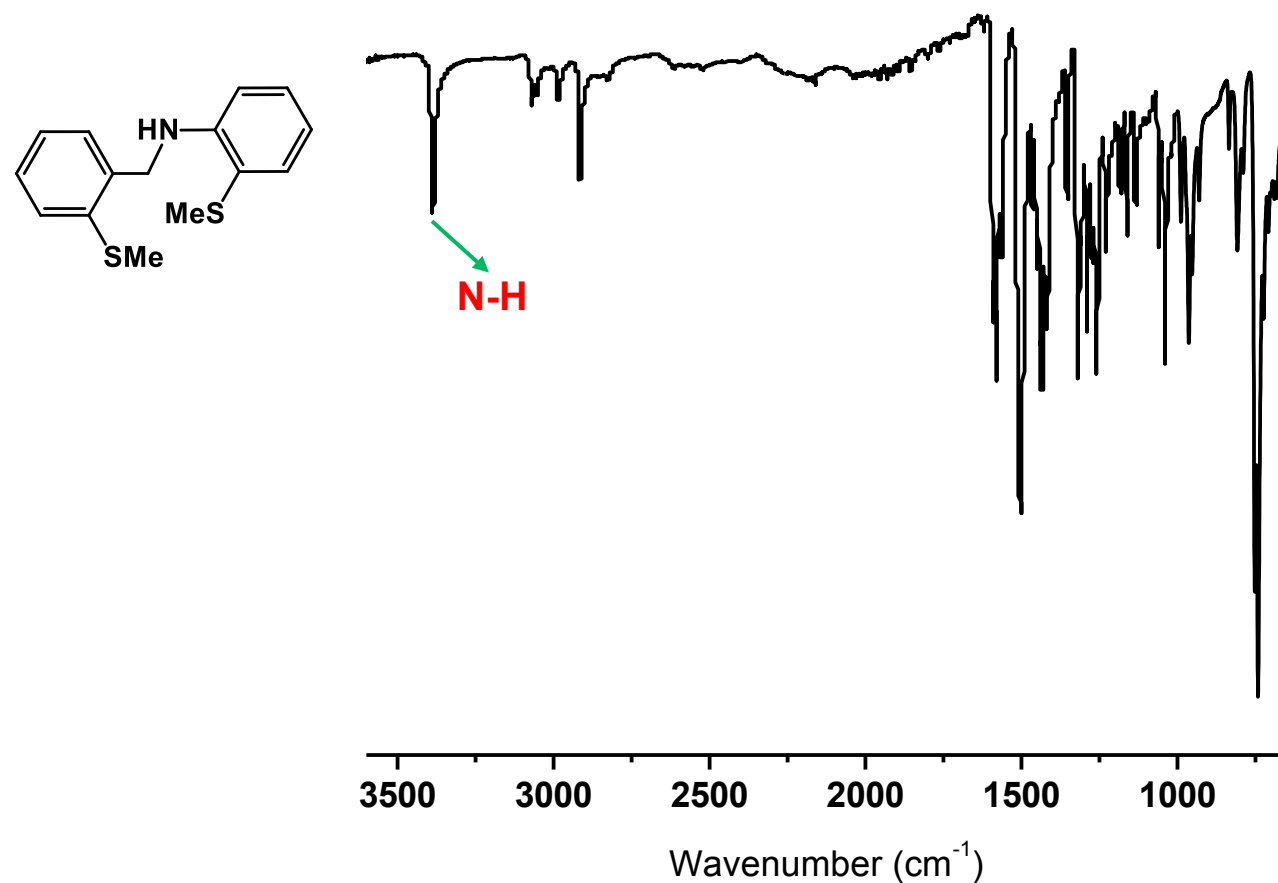


Figure S7. IR (ATR) spectrum of $[S^{Me}N^H S^{Me}]$ ligand.

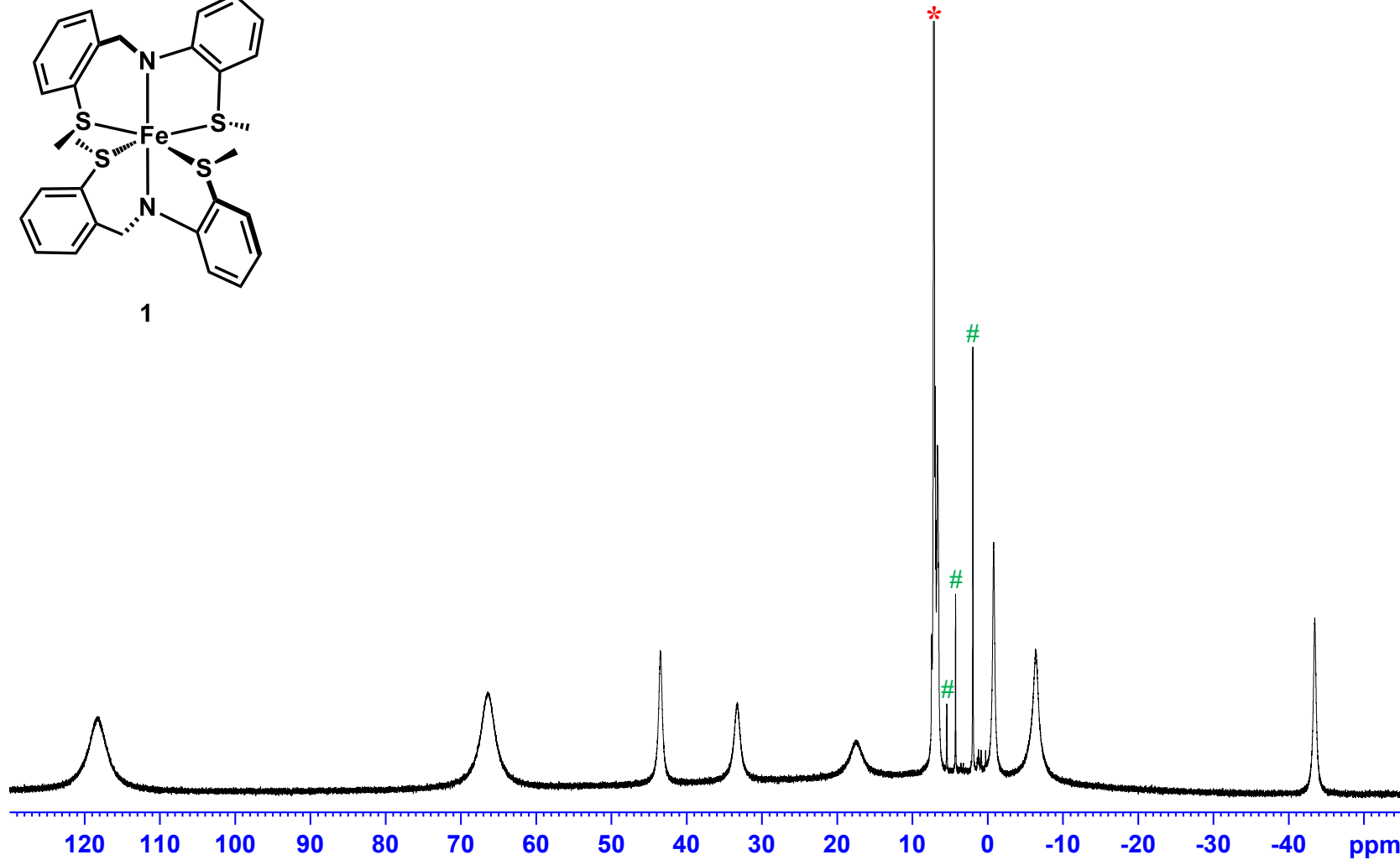
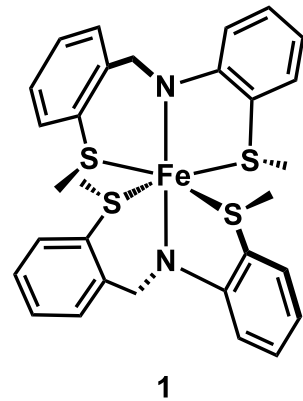


Figure S8. ^1H NMR (300 MHz, C_6D_6) spectrum of $[\text{Fe}(\kappa^3-\text{S}^{Me}\text{NS}^{Me})_2]$ (1) (LB = 1 Hz) [$\#$ = signals of free $[\text{S}^{Me}\text{N}^H\text{S}^{Me}]$ ligand].

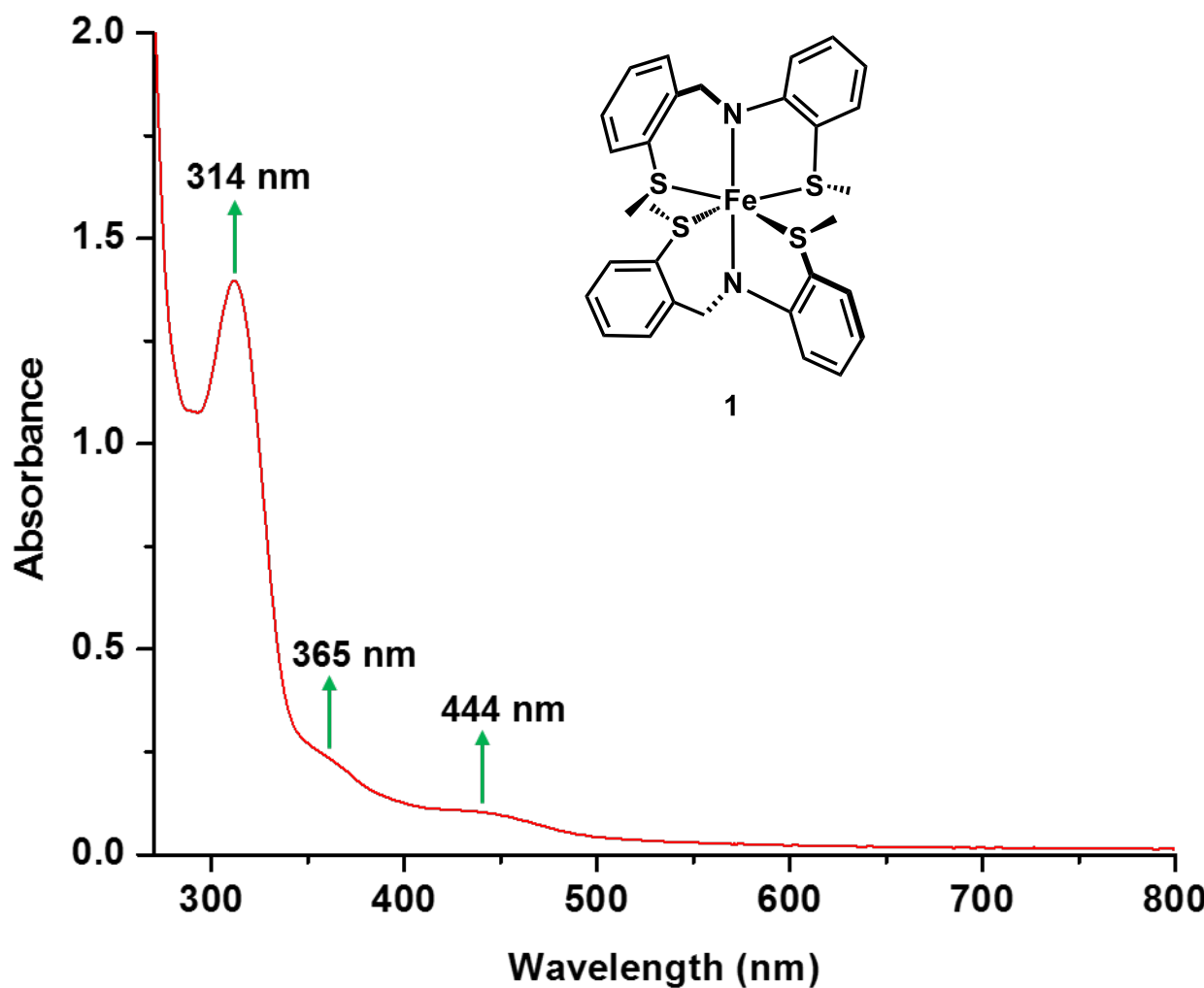


Figure S9. UV-vis spectrum of $[\text{Fe}(\kappa^3\text{-S}^{Me}\text{N}^{Me})_2]$ (**1**) (9.9×10^{-5} M in THF).

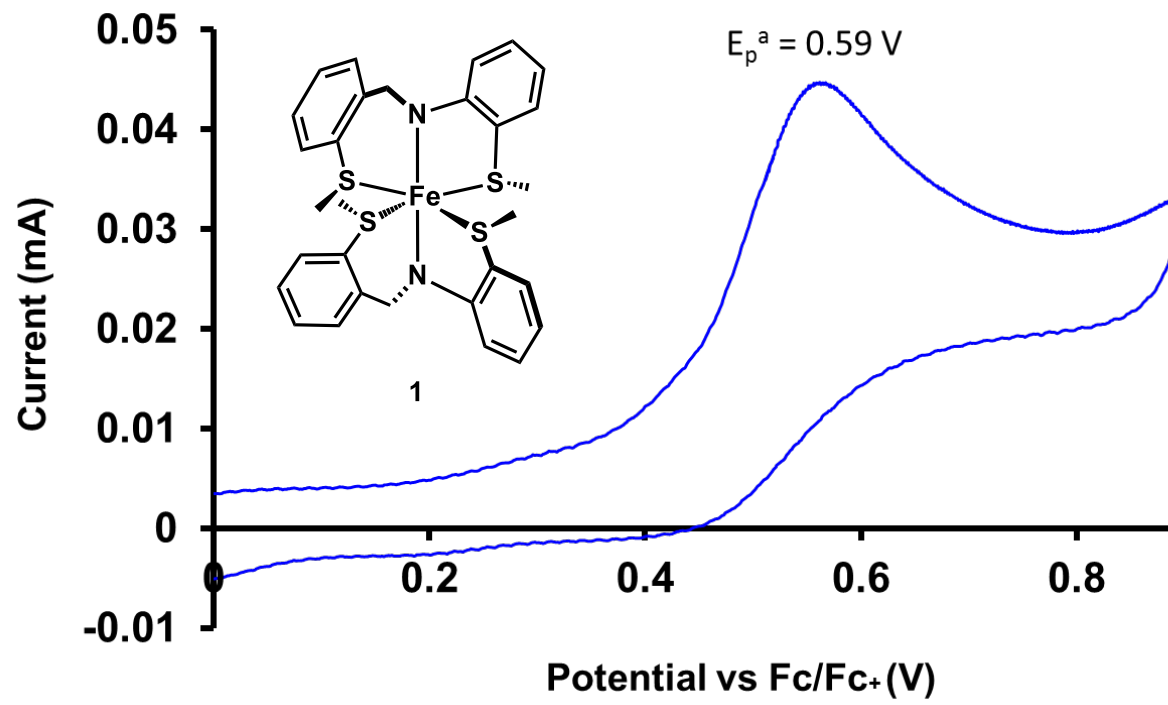


Figure S10. Cyclic voltammogram of $[\text{Fe}(\kappa^3\text{-S}^{Me}\text{N}^{Me})_2]$ (**1**) in CH_2Cl_2 under N_2 atmosphere ([complex] 0.5 mM, at 100 mV scan rate in 0.1 M n-Bu₄NPF₆).

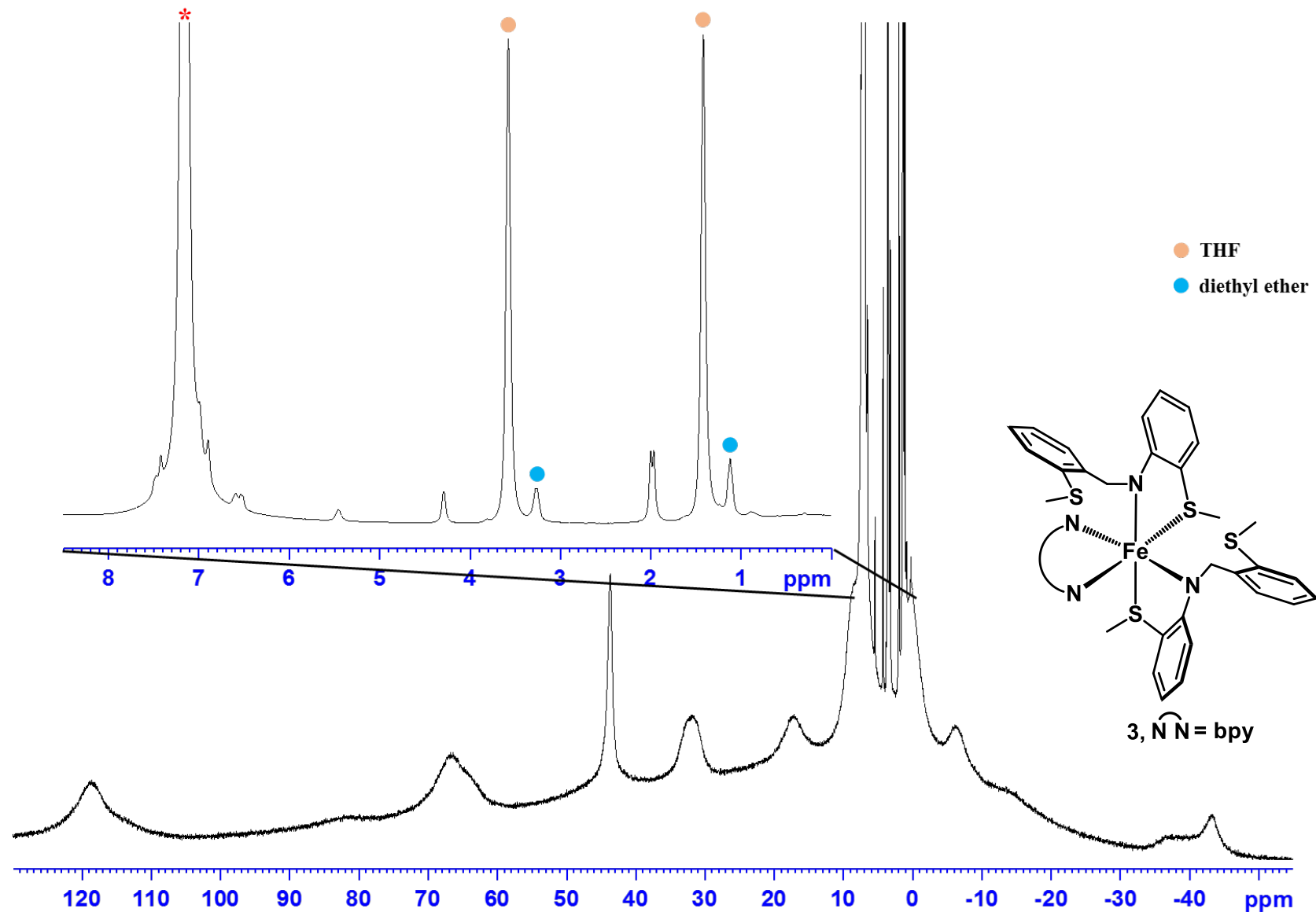


Figure S11. ^1H NMR (300 MHz, C_6D_6) spectrum of $[\text{Fe}(\kappa^3-\text{S}^{Me}\text{N}\text{S}^{Me})_2(\text{bpy})]$ (**3**) (LB = 3 Hz).

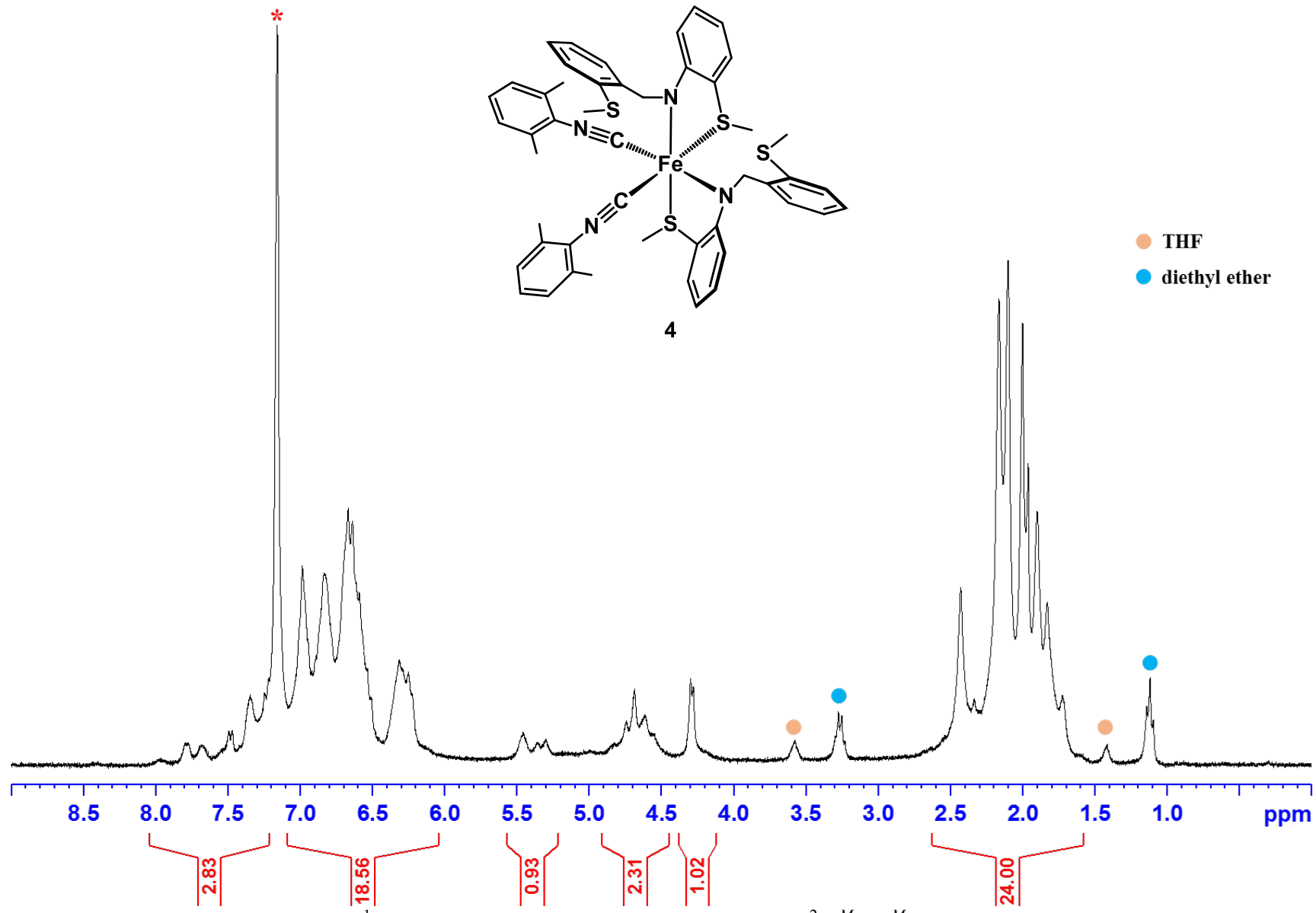


Figure S12. ^1H NMR (300 MHz, C_6D_6) spectrum of $[\text{Fe}(\kappa^2\text{-S}^{Me}\text{NS}^{Me})_2(\text{CNxylyl})_2]$ (**4**).

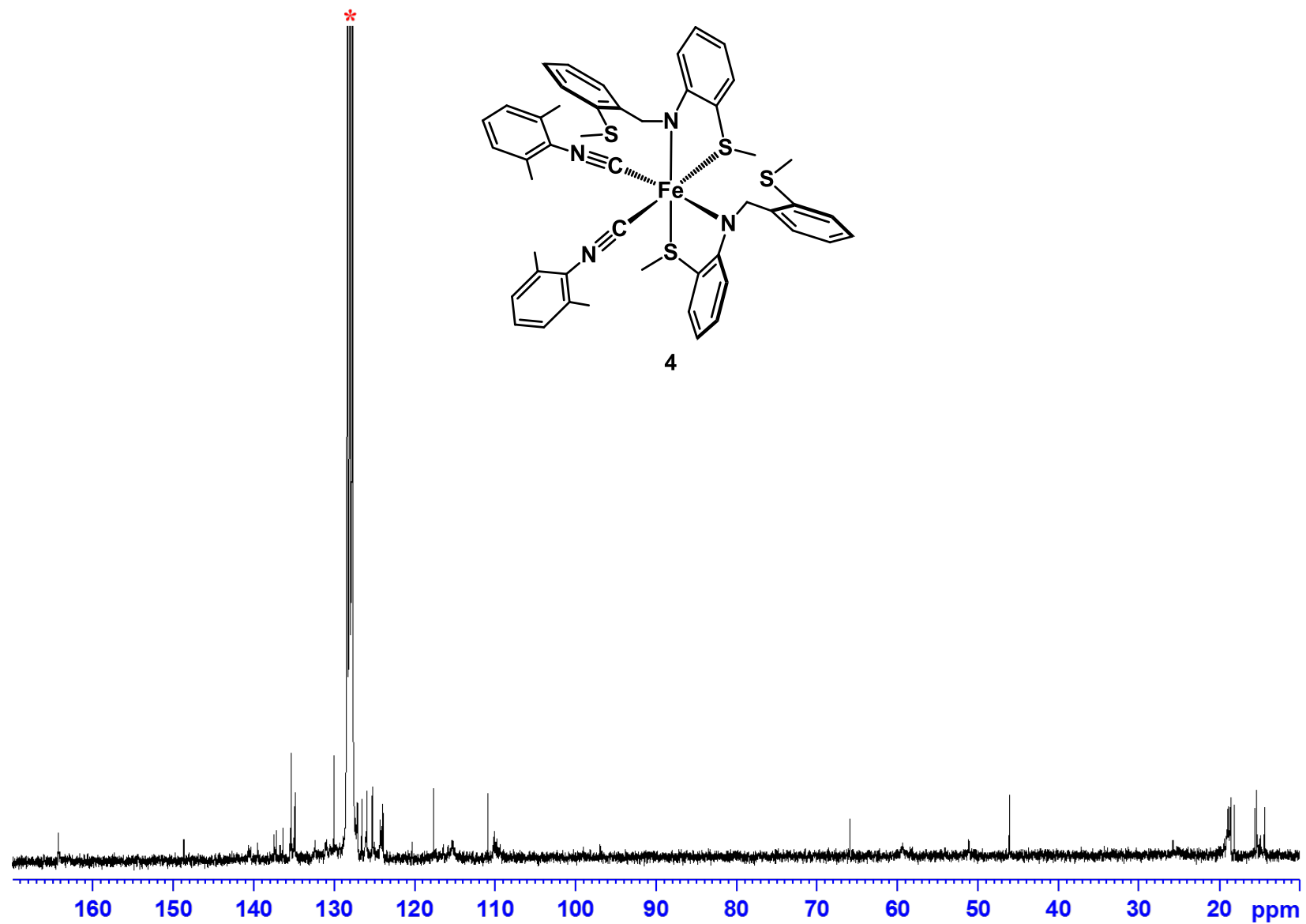


Figure S13. $^{13}\text{C}\{\text{H}\}$ NMR (75 MHz, C_6D_6) spectrum of $[\text{Fe}(\kappa^2\text{-S}^{\text{Me}}\text{NS}^{\text{Me}})^2(\text{CNxylyl})_2]$ (4).

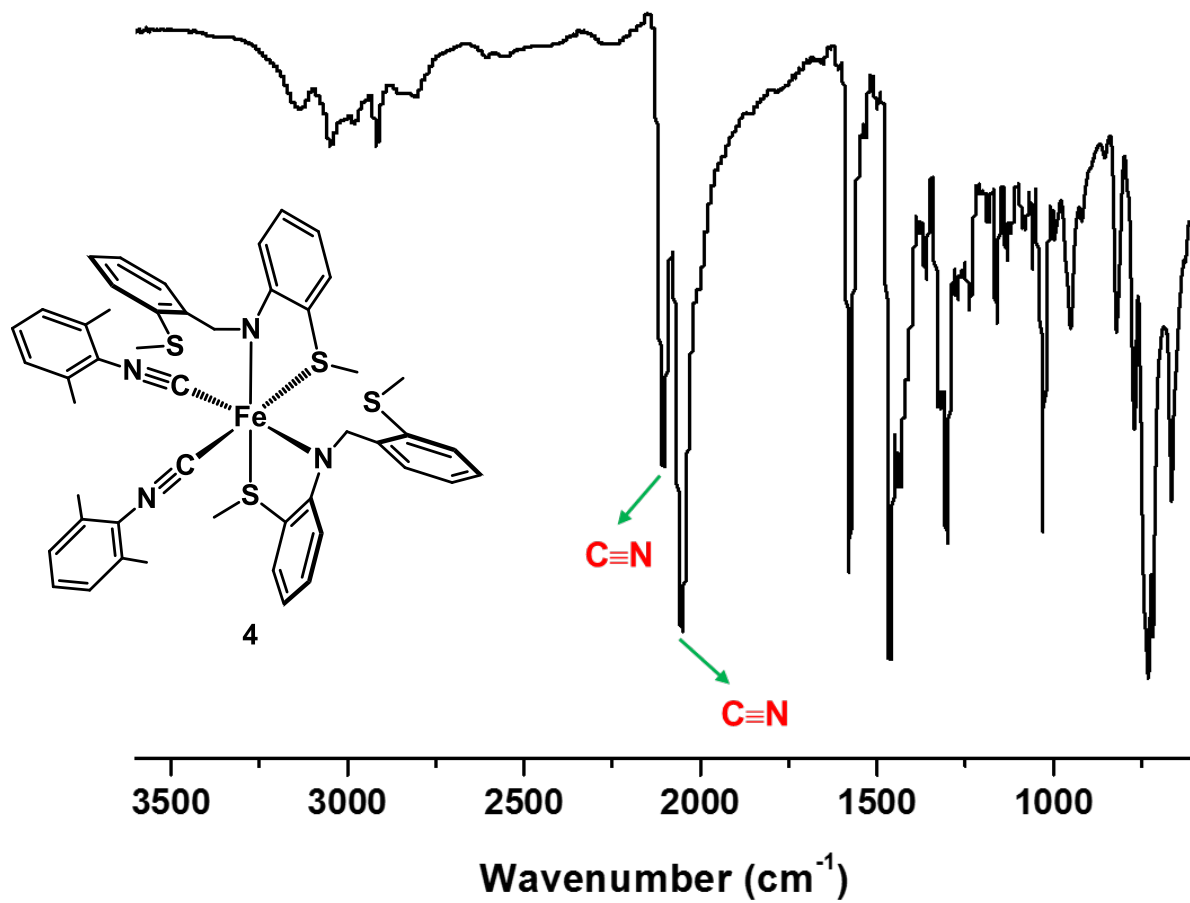


Figure S14. IR (ATR) spectrum of $[Fe(\kappa^2-S^{Me}NS^{Me})_2(CNxylyl)_2]$ (4).

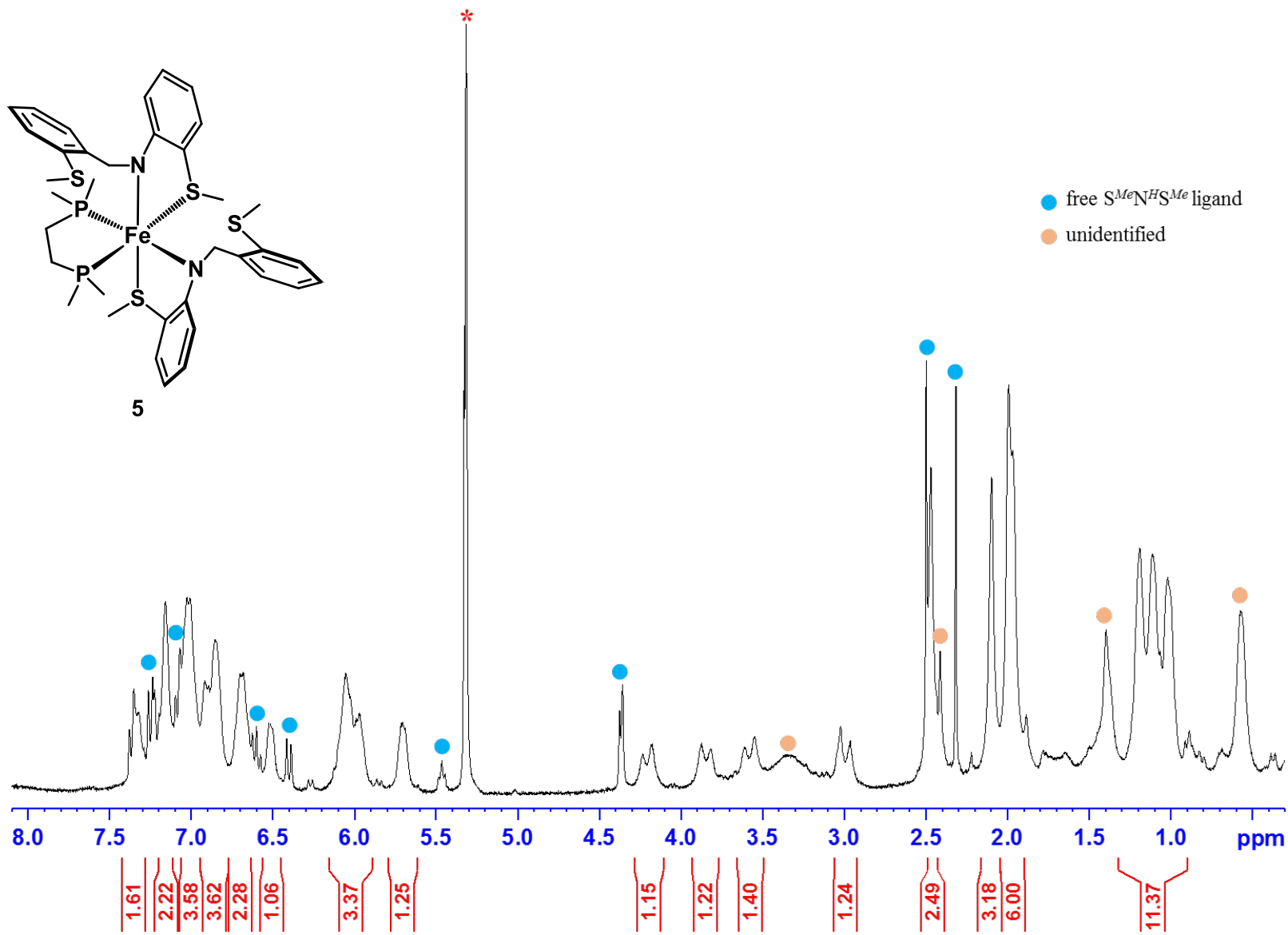


Figure S15. ^1H NMR (300 MHz, CD_2Cl_2) spectrum of $[\text{Fe}(\kappa^3\text{-S}^{\text{Me}}\text{NS}^{\text{Me}})_2(\text{dmpe})]$ (**5**) at -40°C .

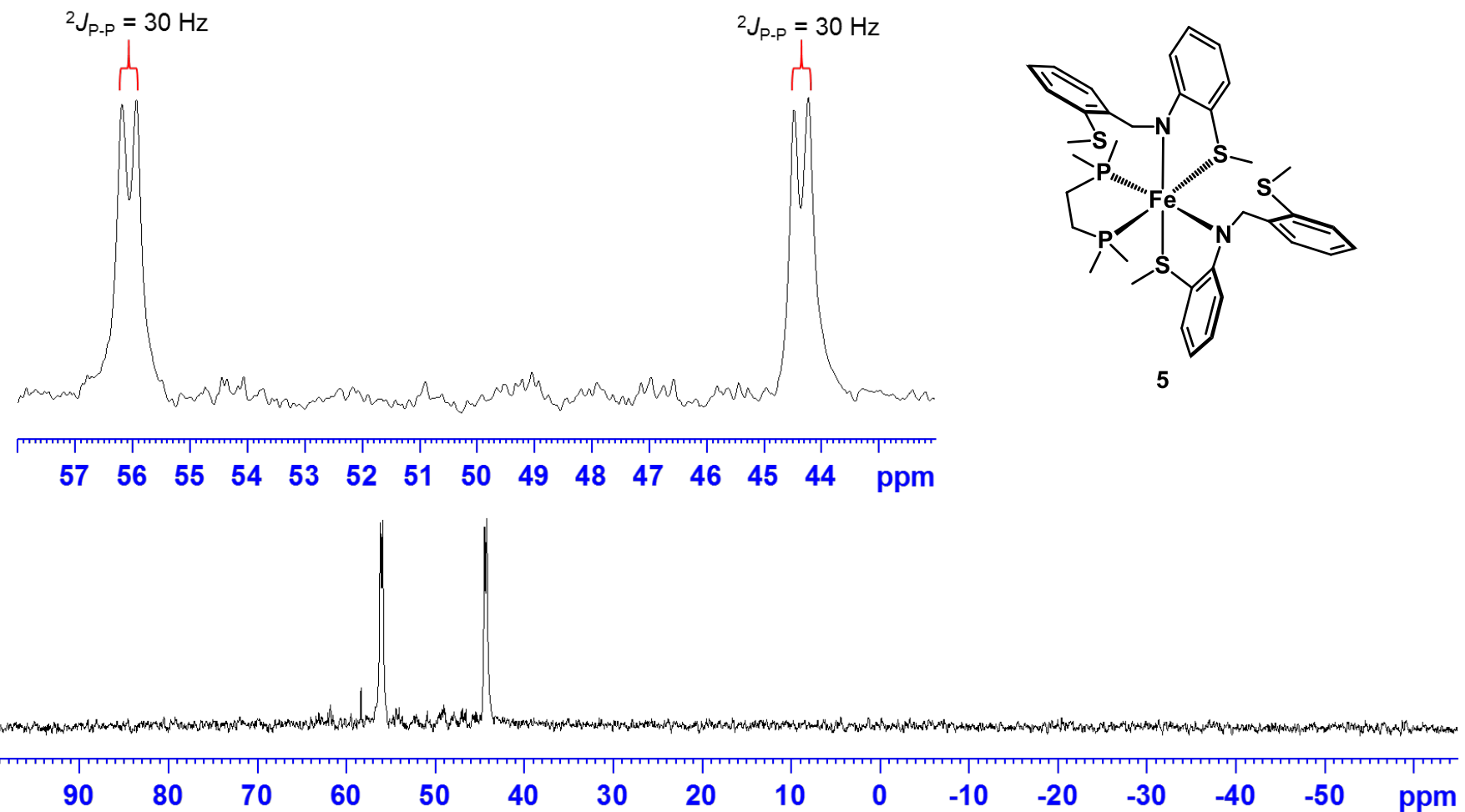


Figure S16. $^{31}\text{P}\{\text{H}\}$ NMR (121 MHz, CD_2Cl_2) spectrum of $[\text{Fe}(\kappa^3\text{-S}^{Me}\text{NS}^{Me})_2(\text{dmpe})]$ (**5**) (LB = 8 Hz) at -40°C.

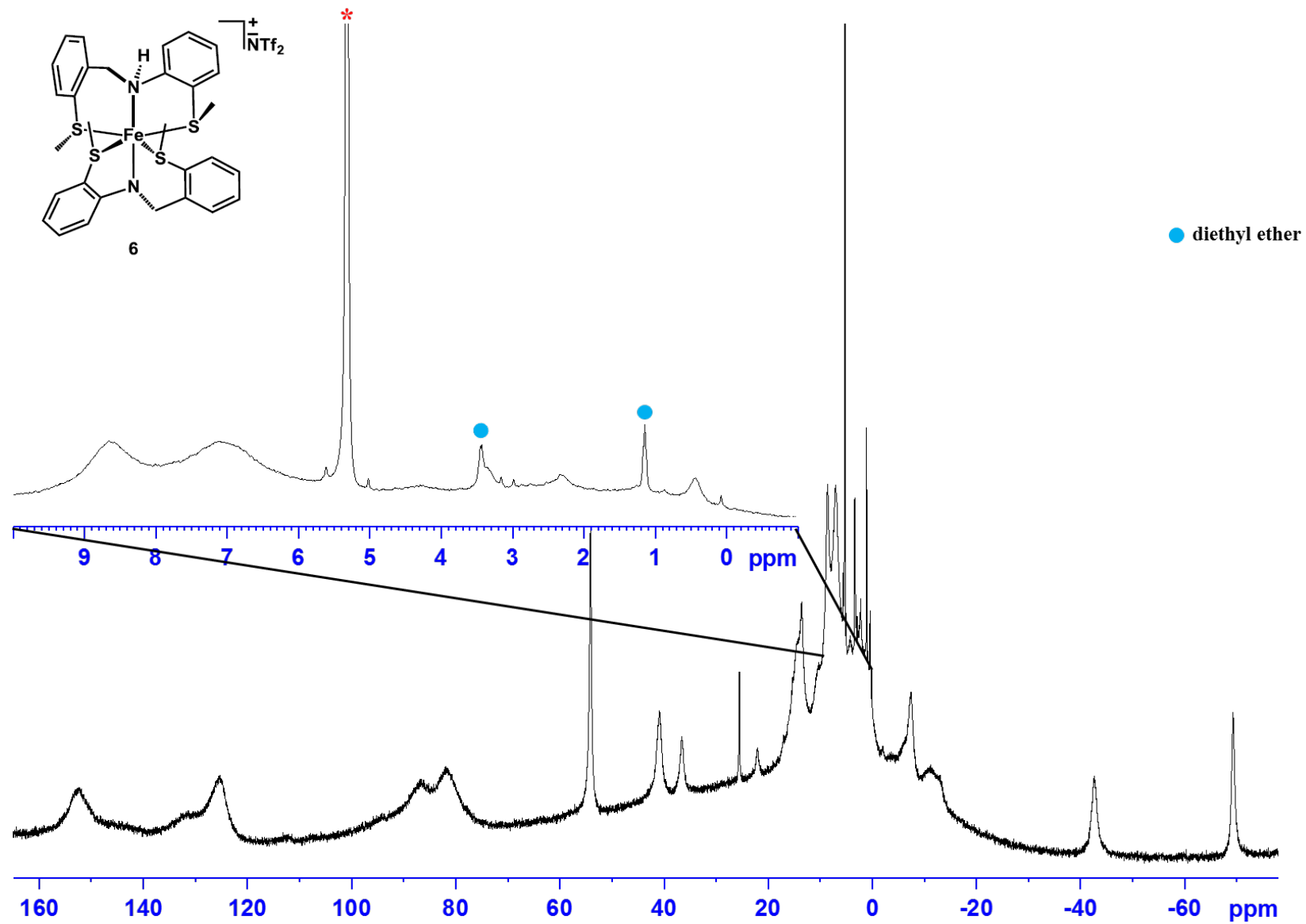


Figure S17. ^1H NMR (300 MHz, CD_2Cl_2) spectrum of $[\text{Fe}(\kappa^3\text{-S}^{Me}\text{NS}^{Me})(\kappa^3\text{-S}^{Me}\text{N}^{\text{H}}\text{S}^{Me})](\text{NTf}_2)$ (**6**).

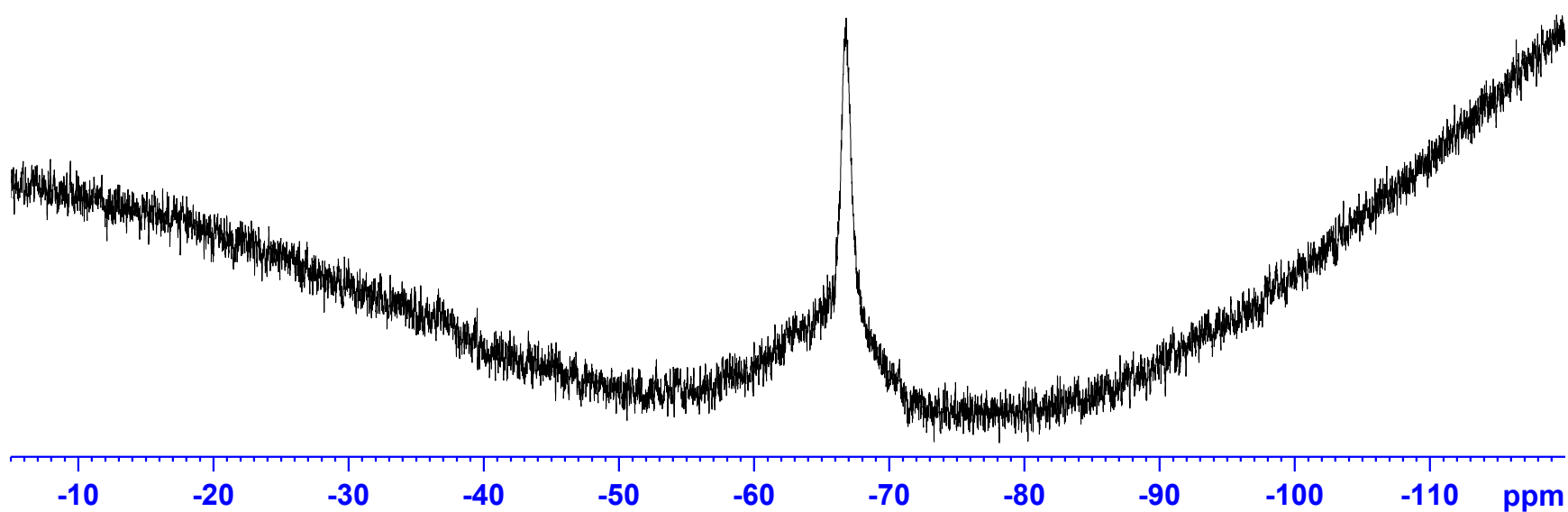
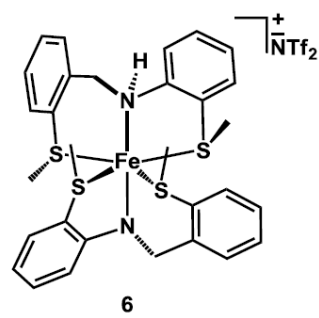


Figure S18. ^{19}F NMR (282 MHz, CDCl_3) spectrum of $[\text{Fe}(\kappa^3\text{-S}^{\text{Me}}\text{NS}^{\text{Me}})(\kappa^3\text{-S}^{\text{Me}}\text{N}^{\text{H}}\text{S}^{\text{Me}})](\text{NTf}_2)$ (**6**) (LB = 5 Hz).

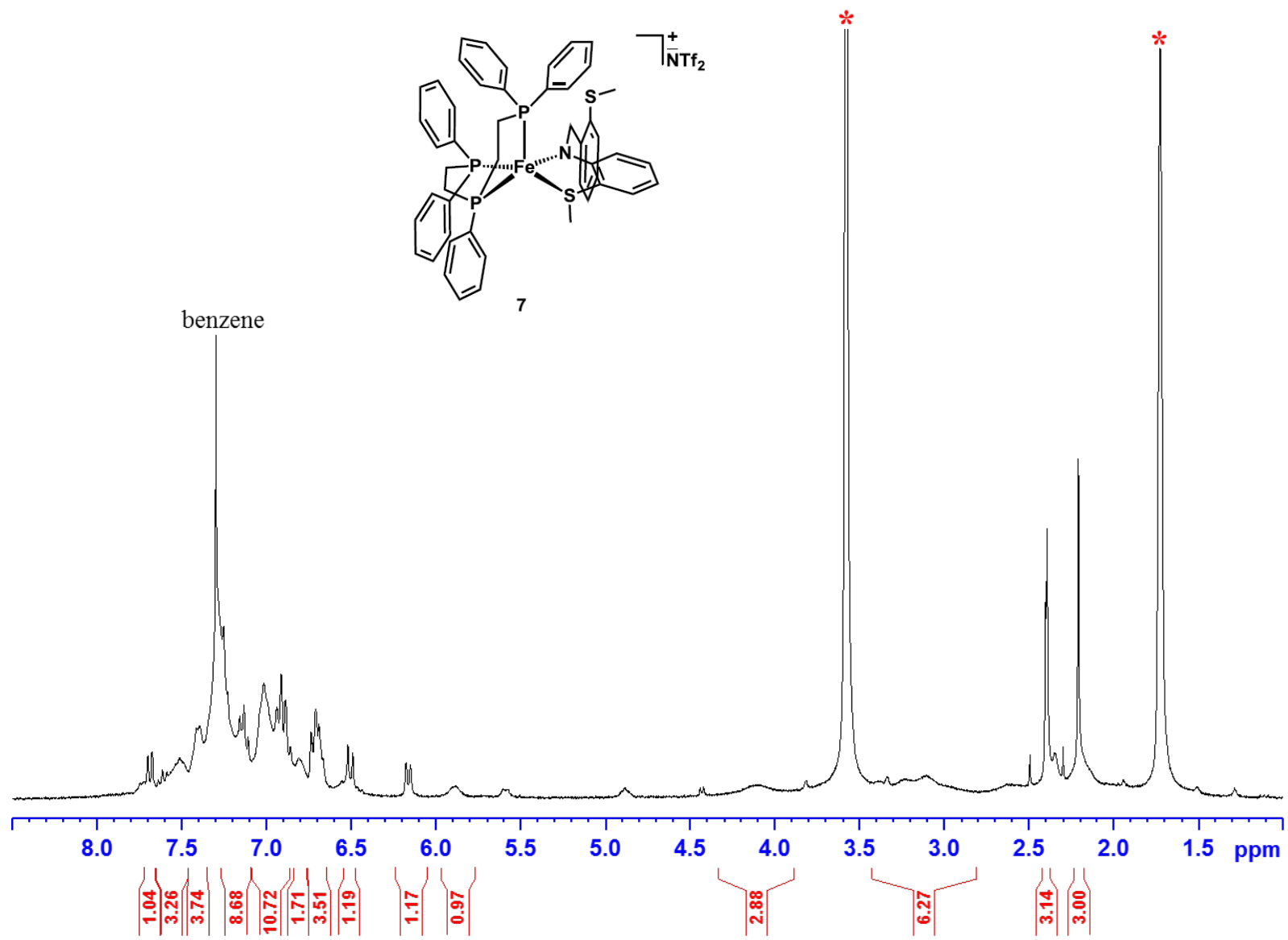


Figure S19. ^1H NMR (300 MHz, THF-d₈) spectrum of $[\text{Fe}(\kappa^2\text{-S}^{Me}\text{NS}^{Me})(\kappa^3\text{-triphos})]$ (**7**) [LB = 0.2 Hz].

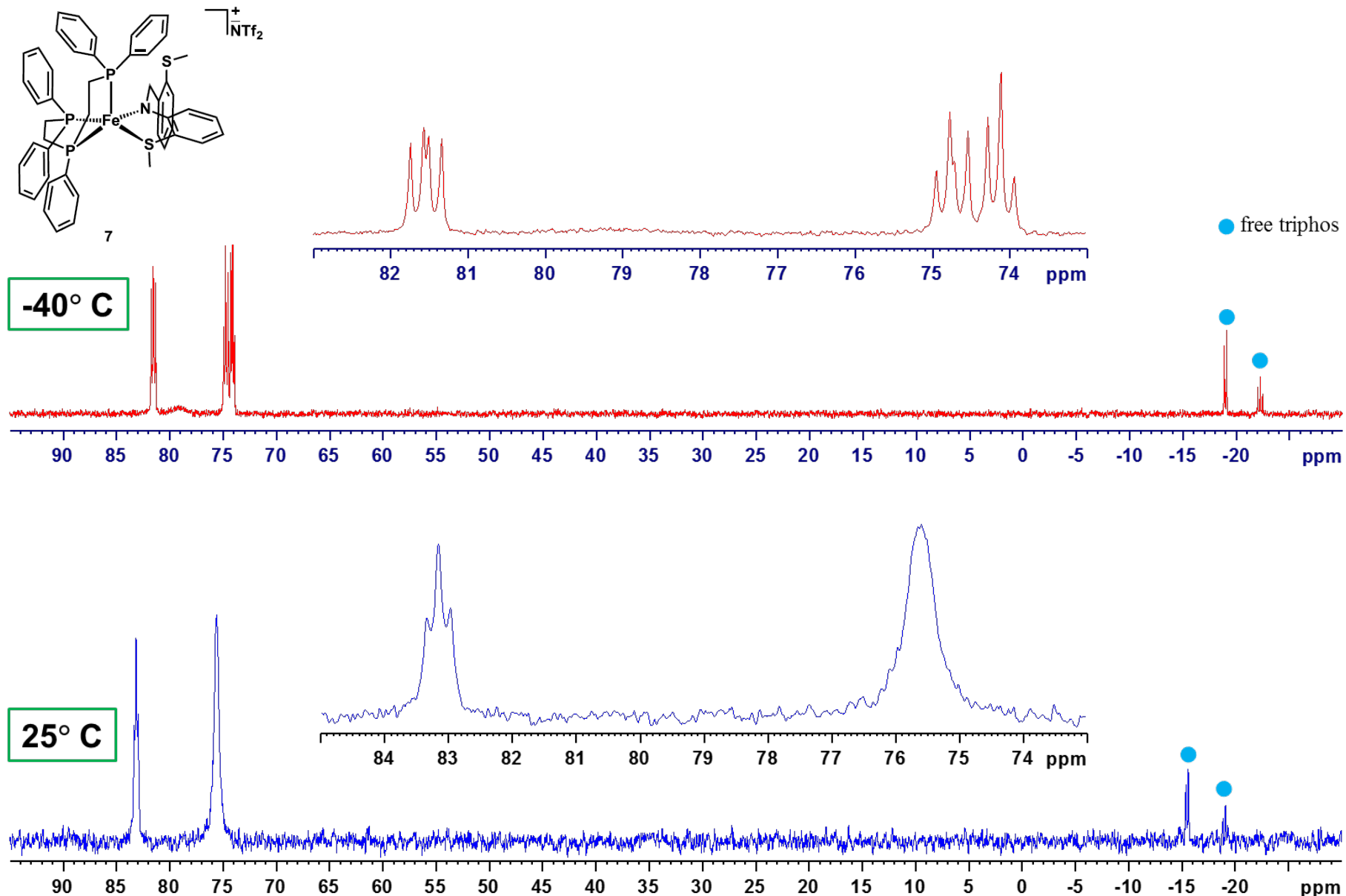


Figure S20. $^{31}\text{P}\{^1\text{H}\}$ NMR (121 MHz, THF-d₈) spectra of $[\text{Fe}(\kappa^2\text{-S}^{\text{Me}}\text{NS}^{\text{Me}})(\kappa^3\text{-triphos})]$ (**7**) [LB = 5 Hz].

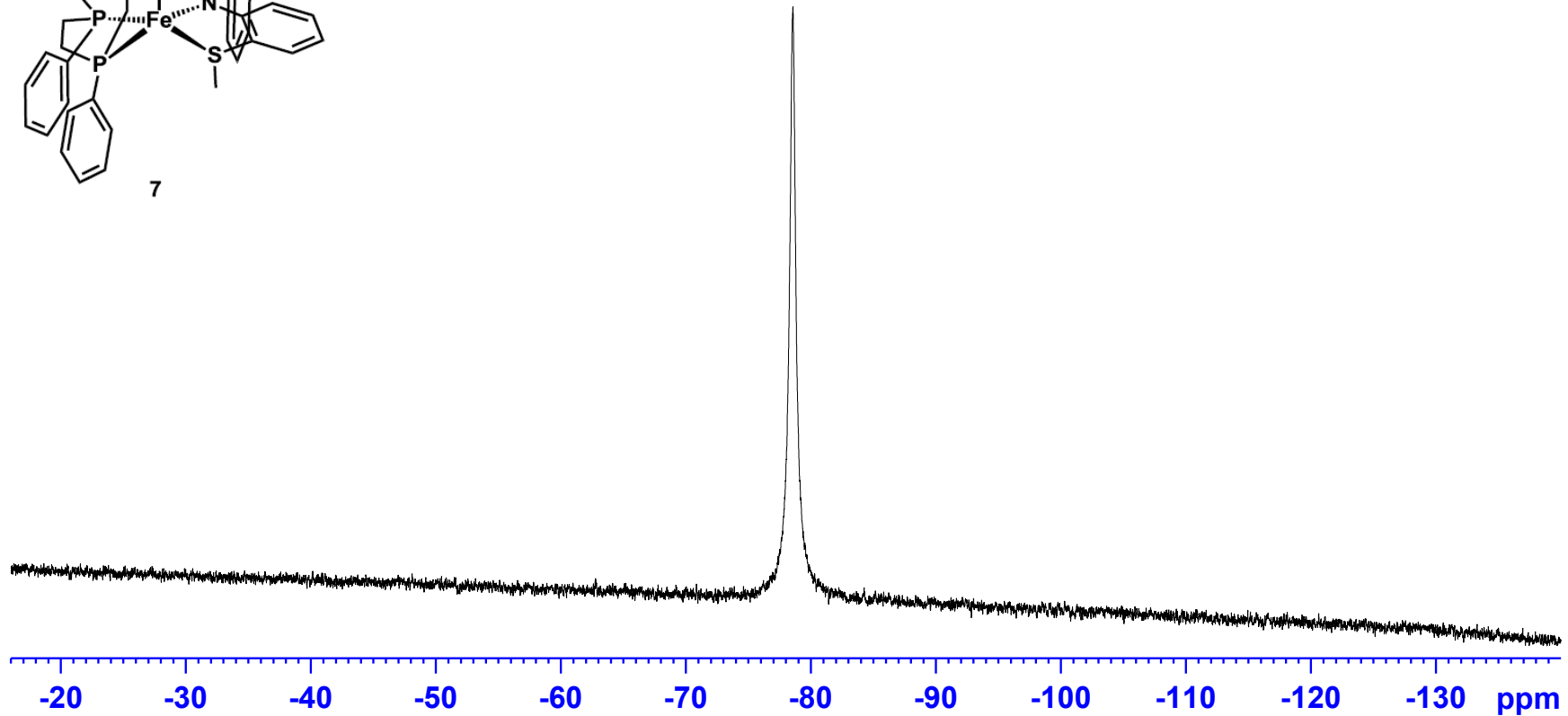
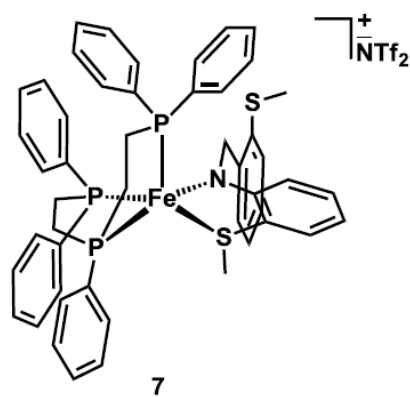
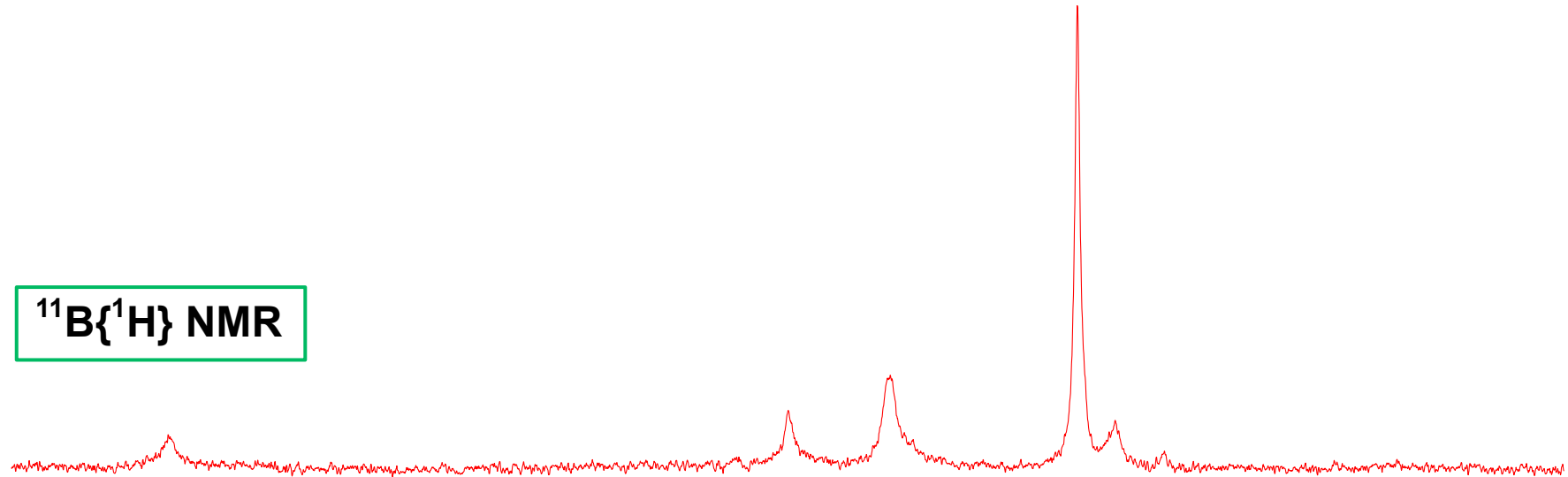


Figure S21. ¹⁹F NMR (282 MHz, THF-d₈) spectrum of [Fe(κ^2 -S^{Me}NS^{Me})(κ^3 -triphos)] (7) (LB = 5 Hz).

$^{11}\text{B}\{\text{H}\}$ NMR



^{11}B NMR

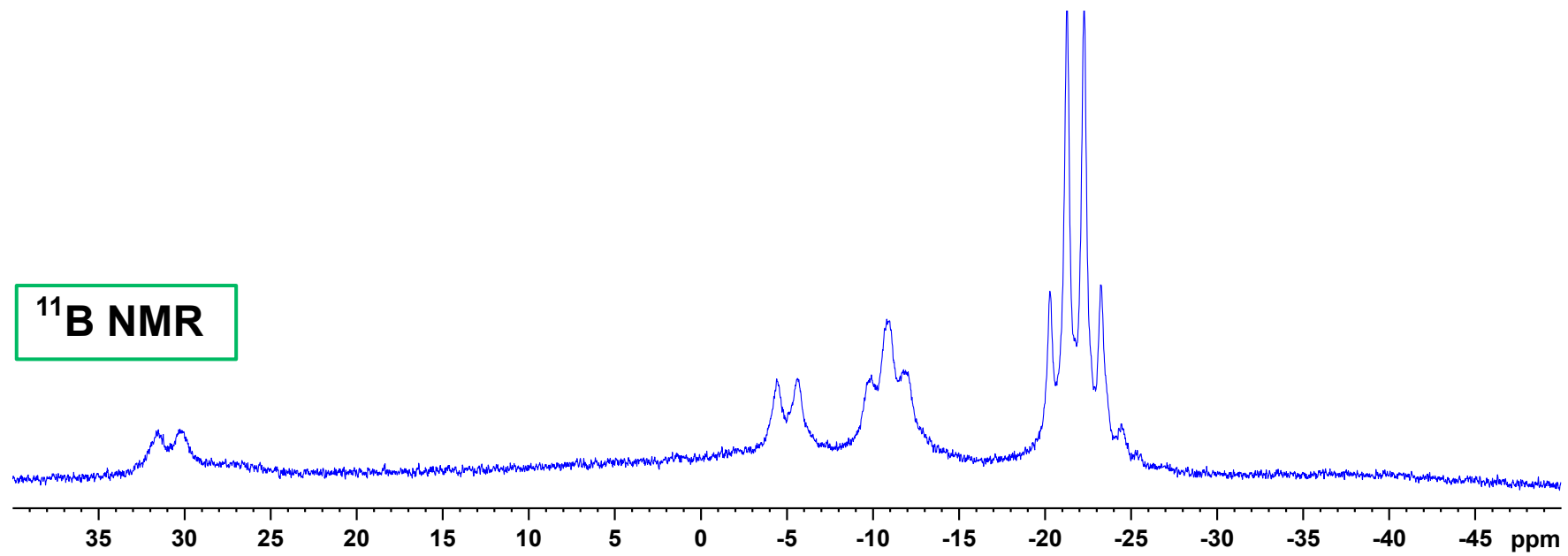


Figure S22. ^{11}B and $^{11}\text{B}\{\text{H}\}$ NMR (96 MHz, THF) spectra of dehydrogenation catalysis of AB with **7** (LB = 3 Hz).

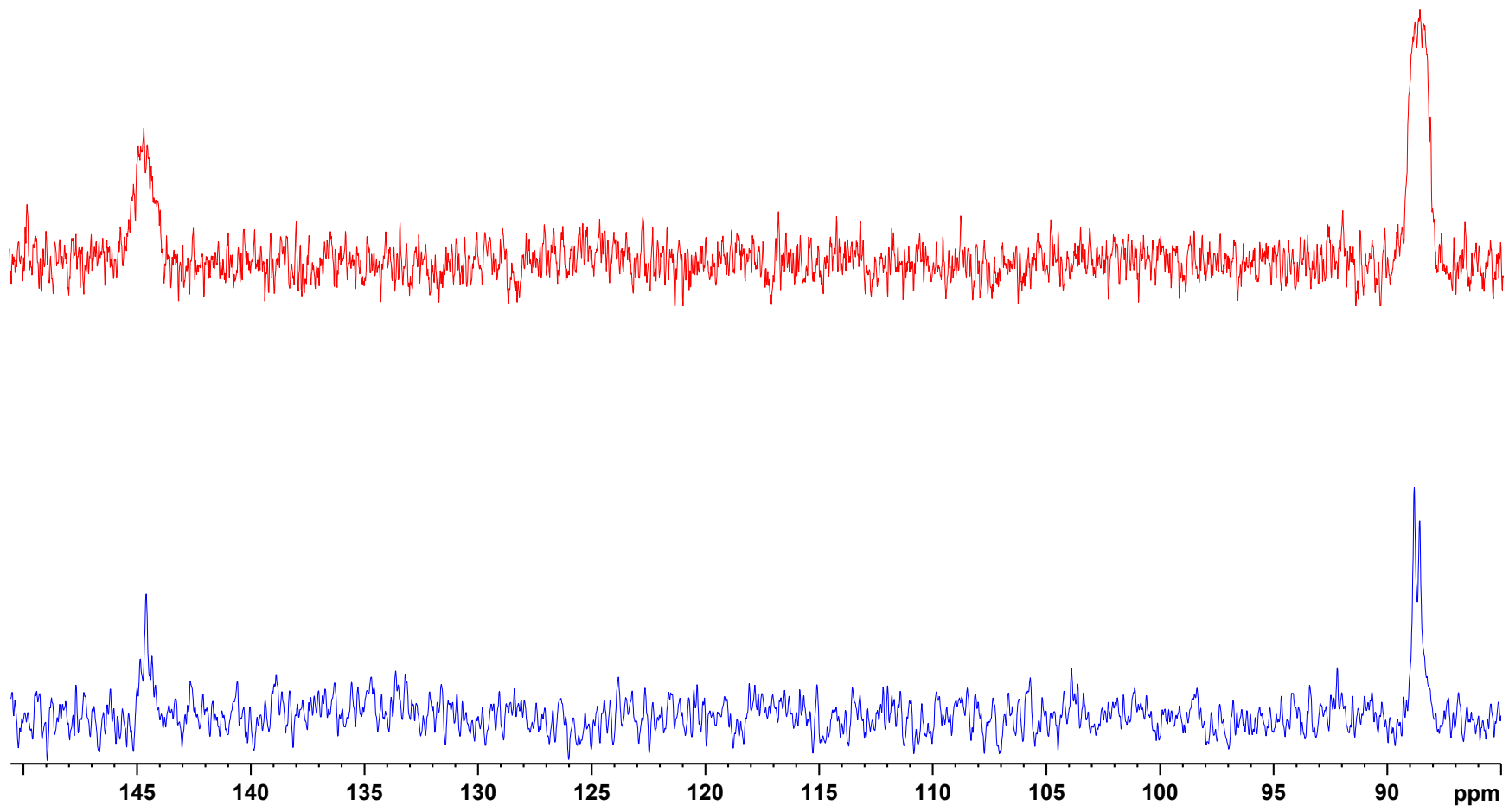


Figure S23. $^{31}\text{P}\{\text{H}\}$ NMR (121 MHz, THF) spectra [Gated ^1H decoupling (top spectrum)] of dehydrogenation catalysis of AB with 7 (LB = 10 Hz).

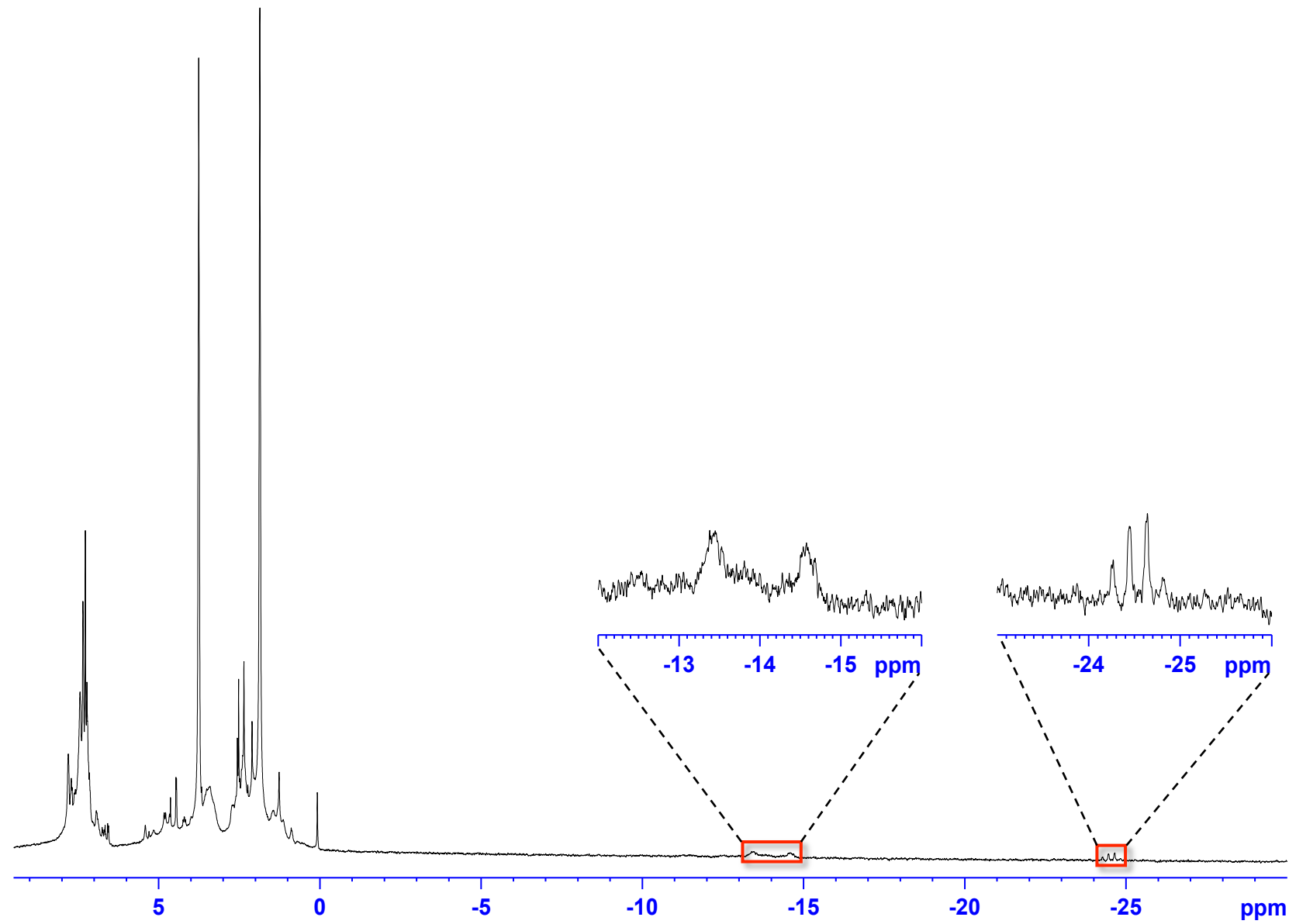


Figure S24. ¹H NMR (300 MHz, CDCl₃) spectrum of dehydrogenation catalysis of AB with 7 (LB = 1 Hz).

$^{11}\text{B}\{\text{H}\}$ NMR

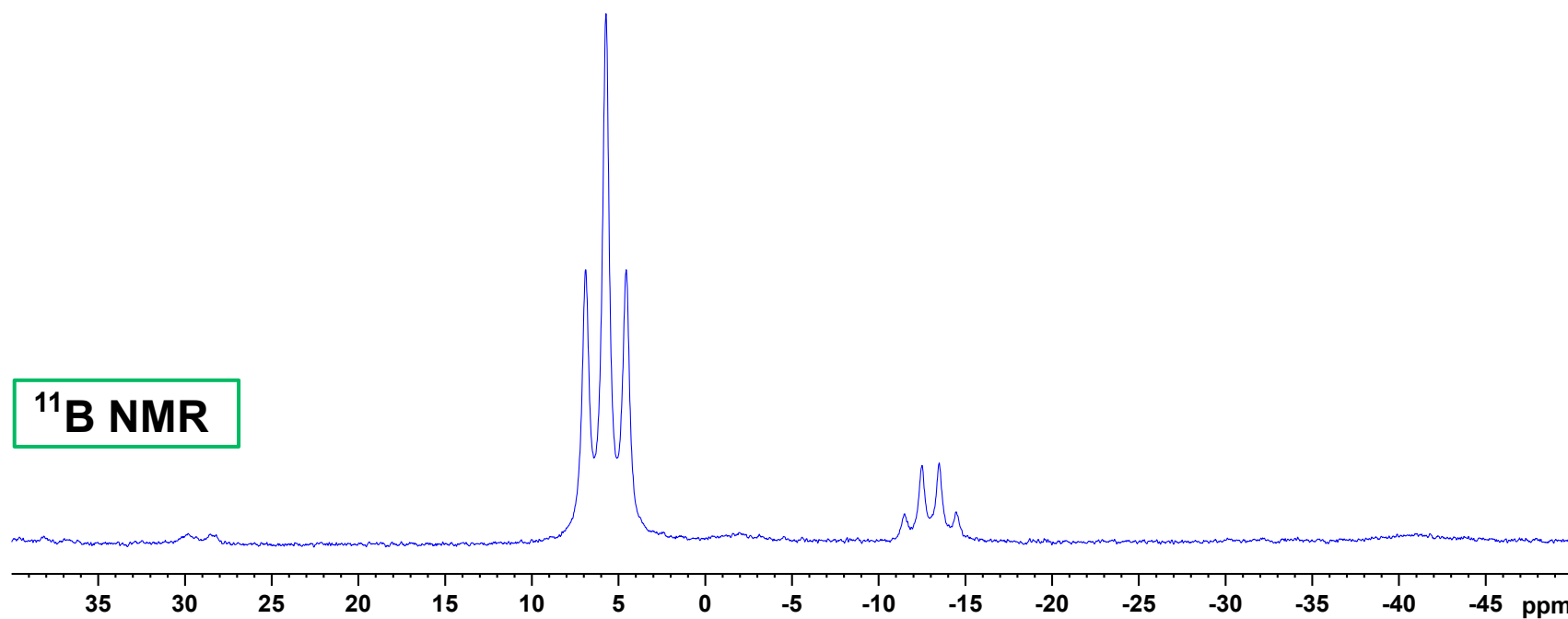


Figure S25. ^{11}B and $^{11}\text{B}\{\text{H}\}$ NMR (96 MHz, THF) spectra of dehydrogenation catalysis of DMAB with 7 (LB = 2 Hz).

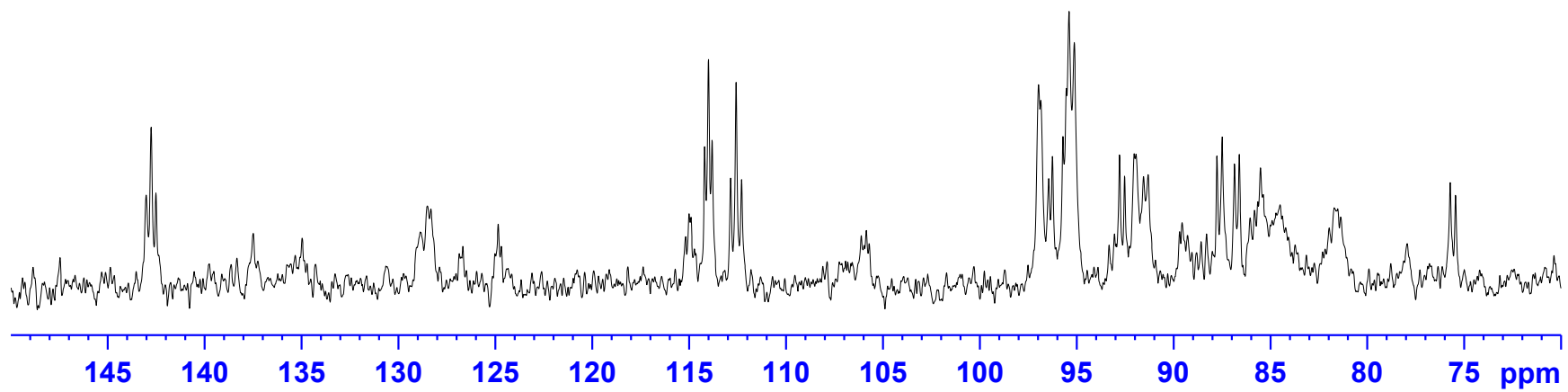


Figure S26. $^{31}\text{P}\{\text{H}\}$ NMR (121 MHz, THF) spectrum of dehydrogenation catalysis of DMAB with **7** (LB = 10 Hz).

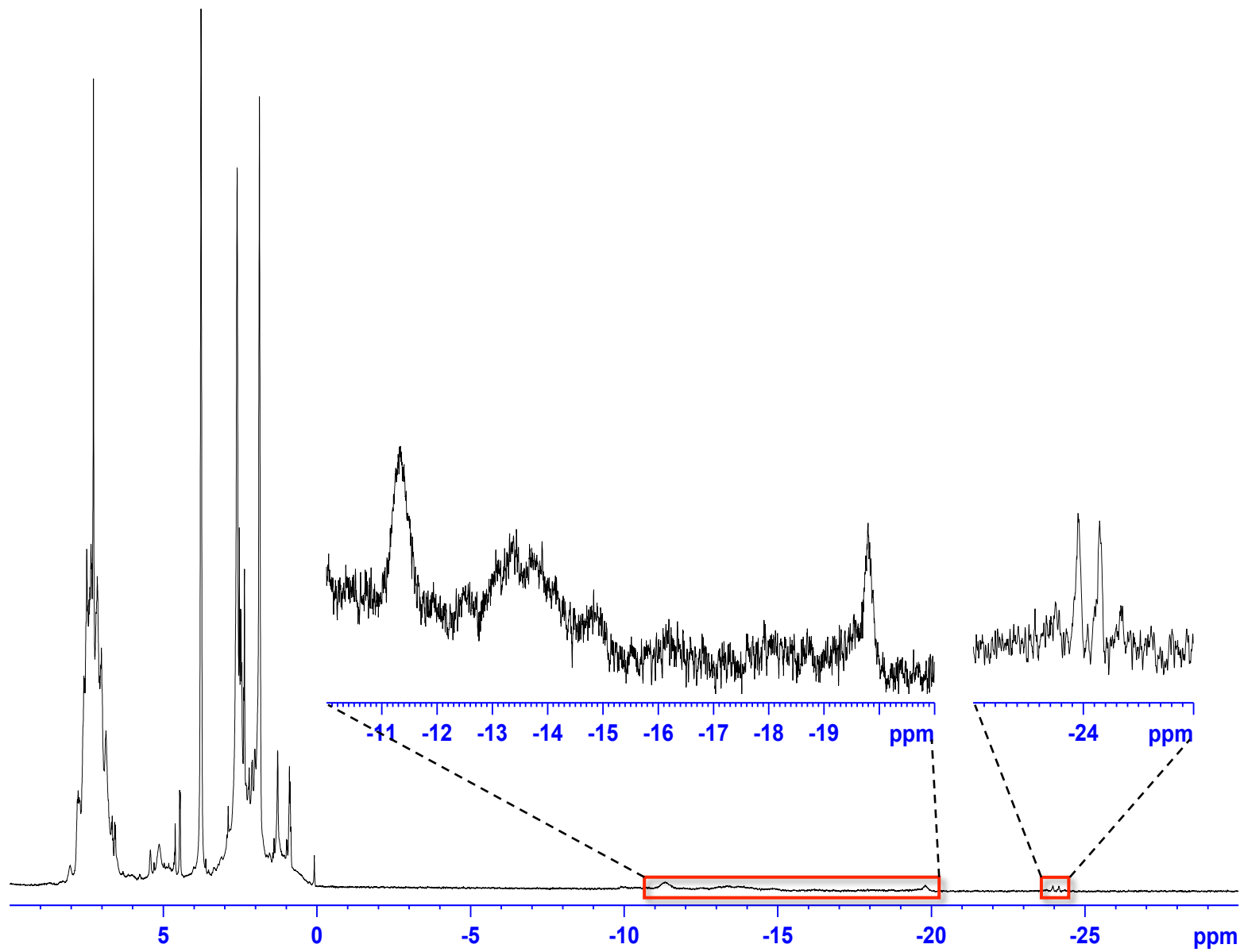


Figure S27. ¹H NMR (300 MHz, CDCl₃) spectrum of dehydrogenation catalysis of DMAB with **7** (LB = 2 Hz).

X-ray crystallography

Experimental. The crystals of **tb081**, **tb148**, **tb149**, and **tb244** were mounted on thin glass fibers using paraffin oil. Prior to data collection, the crystals were cooled to 200(2) K (**tb081**, **tb148**, **tb149**) and 201(2) K (**tb244**). The data were collected on a Bruker AXS single-crystal diffractometer equipped with a sealed Mo tube (wavelength 0.71073 Å) and APEX II CCD detector. The raw data collection and reduction were done with the Bruker APEXII software package.¹ Semi-empirical absorption corrections based on equivalent reflections were applied.² Systematic absences in the diffraction dataset and unit-cell parameters were consistent with monoclinic $P2_1/n$ (#14) for **tb081**, **tb148**, **tb244**, and triclinic $P-1$ (#2) for **tb149**. The structures were solved by direct methods and refined with full-matrix least-squares procedures based on F^2 , using SHELXL³ and WinGX.⁴ All non-H atoms were refined anisotropically. The hydrogen atom H1A bonded to the nitrogen atom in **tb149** was located in a difference Fourier map and refined using a riding model; the remaining hydrogen atoms were placed in idealized positions. In **tb081** no constraints or restraints were applied to the displacement parameters, bond lengths or bond angles. In **tb148** restraints were applied to the displacement parameters for the THF molecule. In **tb149** restraints were applied to the displacement parameters for the trifluoromethyl groups. In **tb244** the Tf₂N anion is disordered over two positions with 0.899(3):0.101(3) occupancies; restraints were applied to the bond distances, bond angles, and displacement parameters of this anion. Bond distance restraints were also applied to the benzene molecule.

Table S1. X-ray diffraction data collection and refinement parameters for complexes **1**, **3**, **6** and **7**.

Parameters	[1]	[3]	[6]NTf ₂	[7]NTf ₂
Formula	C ₃₀ H ₃₂ FeN ₂ S ₄	C ₄₄ H ₄₈ FeN ₄ OS ₄	C ₃₂ H ₃₃ F ₆ FeN ₃ O ₄ S ₆	C ₅₄ H ₅₂ F ₆ FeN ₂ O ₄ P ₃ S ₄
cif ref code	tb081	tb148	tb149	tb244
Fw	604.67	832.95	885.82	1183.97
Color	yellow	red-brown	red	magenta
Temperature/K	200(2)	200(2)	200(2)	200(2)
Crystal system	Monoclinic	Monoclinic	Triclinic	Monoclinic
Space group	P21/n	P21/n	P-1	P21/n
a/Å	11.7737(3)	13.8420(7)	11.2174(3)	18.307(9)
b/Å	15.7702(4)	19.1448(9)	11.6637(3)	15.818(8)
c/Å	15.1996(4)	16.1119(8)	14.6386(4)	18.862(10)
α/deg	90	90	73.989(1)	90
β/deg	101.7320(10)	103.321(2)	89.175(2)	102.417(6)
γ/deg	90	90	85.690(2)	90
V/Å ³	2763.21(12)	4154.8(4)	1835.72(9)	5334(5)
Z	4	4	2	4
Dcal/Mg/m ⁻³	1.453	1.332	1.606	1.474
μ/mm ⁻¹	0.872	0.603	0.825	0.598
F(000)	1264	1752	908	2444
Crystal size/mm	0.15 x 0.13 x 0.10	0.18 x 0.14 x 0.10	0.14 x 0.11 x 0.08	0.81 x 0.71 x 0.08
Reflections collected/unique	44807/6815	65417/10299	24153/8970	41853/9638
θ range/deg	1.88 to 28.33	1.679 to 28.341	1.447 to 28.321	1.697 to 25.247
Index range	-15<=h<=15, -21<=k<=21, -19<=l<=20	-18<=h<=18, -25<=k<=25, -21<=l<=21	-14<=h<=14, -15<=k<=15, -19<=l<=19	-21<=h<=21, -18<=k<=18, -22<=l<=20
R(int)	0.0531	0.0285	0.0264	0.1707
Completeness to θ	28.33, 99.1%	25.242, 99.3%	25.242, 98.6%	25.242, 99.9 %
Max. and min. transmission	0.9179 and 0.8804	0.7457 and 0.6952	0.7457 and 0.6425	0.7456 and 0.5542
Data/restraints/parameters	6815/0/334	10299/60/487	8930/57/469	9638/515/796
Goodness-of-fit on F ²	1.045	1.011	1.064	0.957
R1, wR2 [$\text{I} > 2\sigma(\text{I})$]	0.0489, 0.0950	0.0363, 0.0930	0.0325, 0.0789	0.0635, 0.1327
R1, wR2 (all data)	0.0732, 0.1045	0.0512, 0.0998	0.0448, 0.0846	0.1615, 0.1721

Mössbauer and Magnetic Circular Dichroism (MCD) Spectroscopy

Experimental.

⁵⁷Fe Mössbauer Spectroscopy. Solid state samples were prepared in an inert atmosphere glove box equipped with a liquid nitrogen fill port to enable sample freezing to 77 K within the glovebox. Each sample was loaded into a Delrin Mössbauer sample cup for measurements and loaded under liquid nitrogen. Zero-field ⁵⁷Fe Mössbauer measurements were performed using a See Co. MS4 Mössbauer spectrometer integrated with a Janis SVT-400T He/N₂ cryostat for measurements at 80 K. Isomer shifts were determined relative to α-Fe at 298 K. All Mössbauer spectra were fit using the program WMoss (SeeCo).

Magnetic Circular Dichroism Spectroscopy. The frozen solution MCD sample of **1** was prepared in an inert atmosphere glove box equipped with a liquid nitrogen fill port using 1:1 (v:v) THF:2-MeTHF (a mixture used to afford a low temperature optical glass) in a copper cell fitted with quartz disks and a 3 mm gasket. NIR MCD experiments were conducted using a Jasco J-730 spectropolarimeter and a liquid nitrogen cooled InSb detector. The instrument utilizes a modified sample compartment incorporating focusing optics and an Oxford Instruments SM4000-7T superconducting magnet/cryostat, permitting measurements from 1.6 K to 290 K with magnetic fields up to 7 T. A calibrated Cernox sensor directly inserted in the copper sample holder is used to measure the temperature at the sample to ± 0.001 K. All MCD spectra were baseline-corrected against zero-field scans.

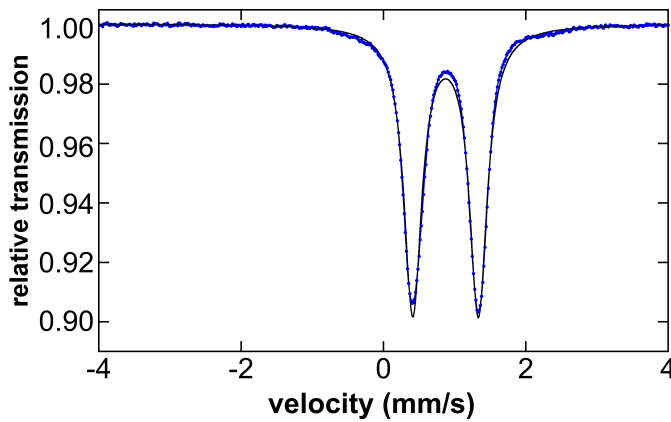


Figure S28. 80 K Mössbauer spectrum of a 3 mM frozen solution of ^{57}Fe -enriched **1** in 1:1 THF/2-MeTHF. The fit to a single major species with $\delta = 0.87 \text{ mm/s}$ and $\Delta E_Q = 0.95 \text{ mm/s}$ gives parameters similar to $[\text{Fe}(\kappa^3\text{-S}^{Me}\text{NS}^{Me})_2]$ (**1**) in the solid-state (see **Table 1**) though with increased line broadening in solution ($\Gamma = 0.30 \text{ mm/s}$). It is important to note that the fit is not ideal across the entire spectrum, indicating the likely presence of a second minor species most likely **2** representing < 3% of total iron.

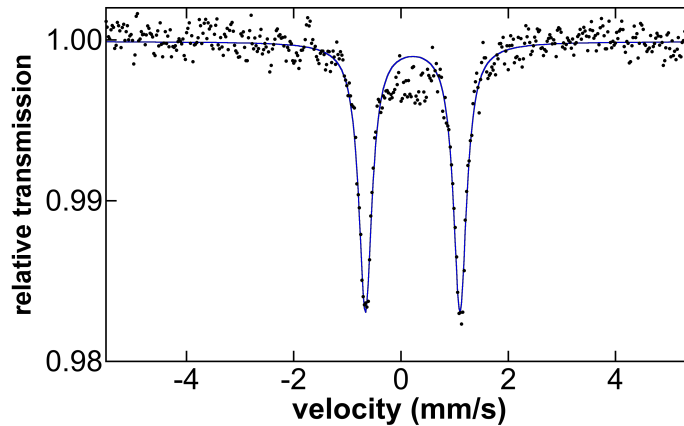


Figure S29. 80 K Mössbauer spectrum of $[\text{Fe}(\kappa^2\text{-S}^{Me}\text{NS}^{Me})(\kappa^3\text{-triphos})](\text{NTf}_2)$ (**7**).

Computational studies

Experimental. Density functional theory (DFT) calculations have been performed using the Gaussian 09 software package (Gaussian Inc., Wallingford, CT).⁵ Optimized molecular geometries were calculated using the PBE^{6,7} exchange-correlation functional in the gas-phase with empirical Grimme's dispersion correction (GD3).⁸ Harmonic frequency calculations were performed to ensure that the stationary points were true energy minima or transition states. The unscaled vibrational frequencies were used for calculating Gibbs free energies of the species at 298 K and 1 atm. TD-DFT calculations were performed with the B3LYP exchange-correlation functional^{9,10} and using the PBE functional-optimized structures. The triple-zeta TZVP¹¹ basis set and tight SCF convergence criteria were used for all calculations. Wave function stability calculations were performed to confirm that the calculated wave functions corresponded to the ground state. Calculations of Mayer bond orders and atomic valences^{12,13} were performed using the AOMix software package.¹⁴

XYZ Atomic coordinates (Å), total electronic energies E(SCF), Gibbs free energies G (at 298K and 1 atm.) and the orbital energies of the highest occupied molecular orbital (HOMO) and the lowest unoccupied molecular orbital (LUMO) for optimized complexes.

Six-coordinate structure 1

E(SCF)= -4126.454334 a.u.

G= -4125.995716 a.u. S**2= 6.021 Annihilated = 6.000

Alpha-spin HOMO= -3.6447 LUMO= -1.4539 Gap= 2.1908 eV

Beta-spin HOMO= -3.2297 LUMO= -2.6093 Gap= 0.6204 eV

Fe	0.389490	0.109473	0.487040
S	-0.803860	2.094922	1.423871
S	1.192312	-2.363822	-0.365953
S	2.204138	0.084830	2.262473
S	-0.836805	0.215018	-1.945974
N	-1.170542	-0.868359	1.360683
N	1.912310	0.997568	-0.525232
C	-2.367899	-0.205269	1.449768
C	-2.377466	1.229833	1.425324
C	-3.559116	1.968075	1.411880
H	-3.492148	3.057305	1.365404
C	-4.803440	1.331267	1.467831
H	-5.726772	1.911328	1.452429
C	-4.826660	-0.064502	1.560966
H	-5.783446	-0.588891	1.625615
C	-3.651610	-0.813071	1.558055
H	-3.730751	-1.896723	1.602571
C	-0.464655	2.055793	3.234724
H	-1.202621	2.676390	3.757116
H	0.545693	2.455301	3.385547
H	-0.508032	1.019105	3.590493
C	-1.180789	-2.328950	1.477096
H	-1.932451	-2.674731	2.208395
H	-0.203697	-2.636898	1.886765
C	-1.406606	-3.041702	0.150477

C	-0.394230	-3.047995	-0.837540
C	-0.635656	-3.602378	-2.101102
H	0.139541	-3.597205	-2.866580
C	-1.878419	-4.173014	-2.390947
H	-2.057469	-4.594230	-3.382090
C	-2.872010	-4.219363	-1.412517
H	-3.836166	-4.684402	-1.624848
C	-2.624480	-3.659835	-0.154911
H	-3.402208	-3.700310	0.610598
C	2.059989	-2.169218	-1.955260
H	2.302114	-3.145753	-2.392120
H	2.986545	-1.634283	-1.712388
H	1.458316	-1.561548	-2.643144
C	3.192300	0.581126	-0.258078
C	3.511991	0.032891	1.027418
C	4.791393	-0.414627	1.344279
H	4.996880	-0.792881	2.347989
C	5.819313	-0.380522	0.394258
H	6.815620	-0.744508	0.647426
C	5.543335	0.150508	-0.868290
H	6.331314	0.196874	-1.623896
C	4.270394	0.620216	-1.191108
H	4.094502	1.002159	-2.196627
C	2.320228	-1.577747	3.028632
H	3.217551	-1.657719	3.653730
H	2.320936	-2.351029	2.250997
H	1.429346	-1.681664	3.661472
C	1.747241	1.761270	-1.764111
H	1.765977	1.094062	-2.655873
H	2.596440	2.456885	-1.889257
C	0.483890	2.592416	-1.805051
C	-0.795074	2.004334	-1.919842
C	-1.946371	2.800533	-1.955038
H	-2.934085	2.345875	-2.021980
C	-1.835256	4.190865	-1.876601

H	-2.739928	4.801746	-1.899781
C	0.562634	3.986398	-1.729228
H	1.549179	4.446506	-1.631310
C	-2.613952	-0.187884	-1.954863
H	-3.081692	0.158486	-2.884990
H	-3.116714	0.226909	-1.073411
H	-2.655095	-1.282803	-1.907414
C	-0.580471	4.789798	-1.763810
H	-0.489646	5.875238	-1.697197

Summary of calculated electronic transitions (TD-DFT):

#	nm	1000 cm ⁻¹	eV	f	Assignment (excitations with contrib. greater than 10.0%)
1	3271.4	3.06	0.379	0.0000	154->158B(36.7%) 155->158B(29.2%) 154->157B(13.8%)
2	1747.0	5.72	0.710	0.0000	154->157B(30.2%) 155->157B(24.3%) 154->158B(13.2%)
3	1110.8	9.00	1.116	0.0000	154->166B(43.6%) 155->166B(34.3%)
4	675.2	14.81	1.836	0.0001	154->165B(30.7%) 155->165B(25.8%)
5	476.8	20.97	2.600	0.0276	156->157B(87.0%)
6	461.6	21.66	2.686	0.0328	156->158B(85.3%)
7	433.0	23.09	2.863	0.0027	155->157B(31.9%) 154->157B(23.4%) 155->158B(14.7%)
8	420.4	23.78	2.949	0.0015	155->158B(27.0%) 154->158B(21.3%) 160->164(14.8%)
9	407.8	24.52	3.040	0.0072	160->164(29.8%) 156->162B(17.3%)
10	400.5	24.97	3.096	0.0022	159->163(17.1%) 155->157B(10.5%)
11	379.9	26.32	3.263	0.0027	156->159B(42.5%)
12	376.8	26.54	3.291	0.0011	160->161(19.0%) 159->161(17.3%)
13	367.9	27.18	3.370	0.0041	156->159B(16.0%) 156->161B(15.9%)
14	364.2	27.46	3.405	0.0031	156->159B(15.6%) 159->161(15.2%)
15	362.6	27.58	3.420	0.0085	159->161(18.7%) 160->168(11.5%)
16	358.6	27.89	3.458	0.0031	159->161(18.2%) 159->167(12.8%)
17	357.8	27.95	3.465	0.0096	156->160B(54.7%) 159->162(12.1%)
18	354.0	28.25	3.502	0.0062	159->162(39.3%) 160->162(17.6%)
19	353.4	28.30	3.508	0.0105	156->161B(14.9%) 160->163(14.4%) 160->161(14.2%)
20	350.1	28.57	3.542	0.0115	160->161(37.0%) 156->161B(12.7%)
21	347.7	28.76	3.566	0.0006	160->162(53.1%) 159->162(20.5%)
22	345.3	28.96	3.590	0.0012	160->163(51.9%)
23	341.4	29.29	3.631	0.0459	155->159B(28.1%) 156->162B(14.1%) 160->164(12.5%)

24 339.9 29.42 3.647 0.0150 155->159B(35.7%) 156->162B(19.9%)
 25 335.1 29.84 3.700 0.0135 159->163(15.9%) 154->159B(13.0%) 156->164B(11.7%)
 26 334.4 29.90 3.707 0.0005 155->160B(25.7%) 156->163B(16.0%) 154->159B(14.0%)
 27 333.4 29.99 3.719 0.0019 156->163B(20.5%) 155->160B(19.7%) 160->165(17.5%)
 28 333.0 30.03 3.723 0.0020 154->159B(29.5%) 156->164B(15.6%) 160->165(15.1%)
 29 331.6 30.16 3.739 0.0000 160->165(52.3%) 156->163B(17.4%) 155->160B(10.4%)
 30 329.2 30.38 3.766 0.0016 158->162(44.7%) 155->161B(16.7%)
 31 328.3 30.46 3.777 0.0063 155->161B(34.3%) 158->162(22.6%)
 32 324.9 30.78 3.816 0.0051 158->163(26.7%) 158->161(25.2%) 156->165B(14.1%)
 33 323.0 30.96 3.839 0.0043 156->165B(18.9%) 159->163(12.6%) 159->165(10.4%)
 34 321.8 31.07 3.852 0.0070 154->160B(60.2%)
 35 321.0 31.16 3.863 0.0086 154->161B(12.1%) 159->165(10.4%) 155->162B(10.2%)
 36 320.7 31.18 3.866 0.0003 154->161B(28.7%) 158->164(10.5%) 155->164B(10.5%)
 37 320.1 31.24 3.874 0.0038 159->165(19.1%) 155->162B(18.4%)
 38 318.5 31.40 3.893 0.0037 160->166(19.1%) 158->163(16.4%) 159->166(14.2%)
 39 317.5 31.50 3.905 0.0045 160->166(26.7%) 158->163(17.1%) 159->165(11.4%)
 40 316.4 31.60 3.918 0.0000 159->164(49.7%) 160->166(16.4%) 159->165(10.8%)

Five-coordinate structure 1

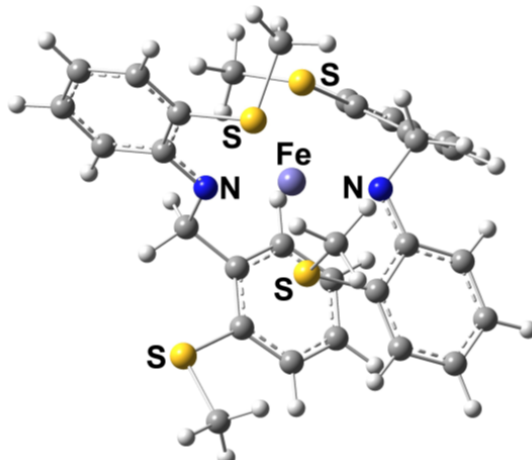
E(SCF)= -4126.449565 a.u.

G= -4125.994468 a.u. S**2= 6.022 Annihilated= 6.000

Alpha-spin HOMO= -3.7372 LUMO= -1.4362 Gap= 2.3010 eV

Beta-spin HOMO= -3.3185 LUMO= -2.6403 Gap= 0.6781 eV

Fe	0.480593	-0.096414	0.628436
S	-0.435592	2.100931	1.435732
S	0.985235	-2.711822	0.001697
S	2.475990	-0.005481	2.116872
S	0.172989	3.699830	-1.965709
N	-1.230291	-0.769464	1.412115
N	1.775515	0.479631	-0.757170
C	-2.322803	0.065432	1.451805
C	-2.120696	1.482435	1.462239
C	-3.178904	2.387129	1.480819



H	-2.955487	3.456678	1.477769
C	-4.503226	1.940485	1.510844
H	-5.330346	2.651290	1.522077
C	-4.734374	0.561354	1.526053
H	-5.759237	0.182192	1.546828
C	-3.682133	-0.351198	1.501122
H	-3.920594	-1.412148	1.485423
C	-0.095052	2.088635	3.248089
H	-0.733179	2.827598	3.747044
H	0.963234	2.344462	3.382278
H	-0.284710	1.083125	3.643578
C	-1.456823	-2.203434	1.624068
H	-2.293908	-2.374264	2.322658
H	-0.562124	-2.608346	2.130014
C	-1.697120	-3.006177	0.352877
C	-0.627476	-3.274518	-0.530898
C	-0.840066	-3.962011	-1.731481
H	-0.010920	-4.167105	-2.409171
C	-2.125532	-4.397434	-2.065921
H	-2.285973	-4.925528	-3.007767
C	-3.188695	-4.174303	-1.190075
H	-4.190279	-4.530852	-1.436422
C	-2.963146	-3.491316	0.008977
H	-3.795719	-3.330468	0.697392
C	2.015511	-2.794916	-1.498700
H	2.237350	-3.834982	-1.767012
H	2.943249	-2.269168	-1.240231
H	1.537193	-2.269448	-2.334571
C	3.125878	0.415807	-0.554110
C	3.647083	0.136355	0.751331
C	5.016438	0.068377	0.999894
H	5.368210	-0.104703	2.019753
C	5.942063	0.224018	-0.036846
H	7.011773	0.158932	0.164709
C	5.464084	0.488558	-1.324856

H	6.168813	0.626593	-2.148383
C	4.099127	0.586715	-1.582185
H	3.768205	0.796947	-2.598999
C	2.903448	-1.649725	2.823869
H	3.914632	-1.626165	3.246468
H	2.817884	-2.432616	2.062062
H	2.178389	-1.836422	3.626913
C	1.312318	0.837862	-2.093043
H	1.604272	0.070180	-2.841541
H	1.783275	1.780700	-2.428913
C	-0.194841	0.973842	-2.104010
C	-0.845390	2.227714	-2.015371
C	-2.247577	2.273405	-1.972982
H	-2.766853	3.227630	-1.893565
C	-3.002655	1.099350	-2.013501
H	-4.090332	1.162694	-1.948020
C	-0.978227	-0.186157	-2.162766
H	-0.478552	-1.152749	-2.243165
C	-0.984028	4.956335	-1.324412
H	-1.411714	4.624948	-0.368571
H	-1.777340	5.200661	-2.042972
H	-0.373003	5.852000	-1.155083
C	-2.373001	-0.140332	-2.110758
H	-2.951261	-1.065092	-2.132464

Summary of calculated electronic transitions (TD-DFT):

#	nm	1000 cm ⁻¹	eV	f	Assignment (excitations with contrib. greater than 10.0%)
1	2729.7	3.66	0.454	0.0000	154->158B(40.2%) 154->157B(26.2%)
2	1755.9	5.70	0.706	0.0002	154->157B(27.9%) 154->158B(25.3%)
3	1198.9	8.34	1.034	0.0002	154->166B(32.1%) 154->161B(11.1%)
4	703.0	14.22	1.764	0.0002	154->161B(22.8%) 154->165B(21.0%) 154->166B(13.2%)
5	480.2	20.82	2.582	0.0236	156->157B(78.2%) 155->157B(13.1%)
6	460.7	21.71	2.691	0.0460	156->158B(61.8%) 155->158B(19.0%)
7	445.6	22.44	2.782	0.0052	155->157B(33.7%) 156->158B(20.6%) 155->158B(18.3%)
8	430.6	23.22	2.879	0.0018	155->158B(38.3%) 155->157B(19.2%)

9	409.2	24.44	3.030	0.0087	160->163(46.6%)	156->162B(10.2%)	
10	402.9	24.82	3.077	0.0014	159->164(29.5%)	156->159B(10.4%)	
11	378.6	26.41	3.275	0.0022	156->161B(19.1%)	156->159B(14.7%)	156->160B(12.3%)
12	374.7	26.69	3.309	0.0031	159->162(19.9%)	156->161B(13.0%)	
13	367.6	27.21	3.373	0.0002	157->166(10.4%)		
14	366.0	27.32	3.388	0.0011	156->160B(12.1%)	157->166(10.8%)	
15	363.7	27.49	3.409	0.0050	155->161B(25.9%)	155->159B(17.5%)	
16	362.2	27.61	3.423	0.0152			
17	357.9	27.94	3.464	0.0029	159->161(49.4%)		
18	356.8	28.03	3.475	0.0172	159->162(24.8%)	156->159B(17.1%)	156->160B(11.1%)
19	354.4	28.22	3.499	0.0046			
20	350.0	28.57	3.542	0.0072	156->161B(27.6%)	156->160B(27.6%)	160->161(11.6%)
21	346.6	28.85	3.577	0.0048	160->161(52.6%)		
22	344.1	29.06	3.603	0.0025	160->162(66.2%)	159->162(17.7%)	
23	341.8	29.25	3.627	0.0432	156->162B(50.0%)	160->163(20.3%)	
24	335.9	29.77	3.691	0.0084	155->159B(49.5%)		
25	334.0	29.94	3.712	0.0007	159->163(68.1%)	160->163(10.9%)	
26	333.6	29.98	3.717	0.0013	153->157B(84.1%)		
27	330.3	30.27	3.753	0.0057	160->165(16.5%)	156->163B(12.8%)	158->162(12.3%)
28	328.8	30.41	3.770	0.0096	160->165(38.1%)	156->163B(13.8%)	160->166(12.3%)
29	327.8	30.50	3.782	0.0199	156->164B(20.7%)	155->160B(18.4%)	158->162(11.2%)
30	326.5	30.63	3.798	0.0045	153->158B(40.0%)	154->159B(13.3%)	
31	325.1	30.76	3.814	0.0006	153->158B(37.3%)	154->159B(11.4%)	156->164B(11.2%)
32	323.9	30.87	3.828	0.0032	160->164(26.4%)	158->162(17.6%)	
33	323.4	30.92	3.834	0.0002	159->165(68.1%)		
34	322.6	31.00	3.843	0.0003	154->160B(18.5%)	156->164B(17.0%)	154->159B(14.6%)
35	321.9	31.07	3.852	0.0057	154->159B(13.0%)	154->162B(12.9%)	155->162B(12.6%)
36	320.8	31.17	3.865	0.0015	160->164(32.6%)	158->162(18.9%)	
37	318.9	31.36	3.888	0.0033	157->165(12.8%)	159->166(10.2%)	
38	317.8	31.47	3.901	0.0044	159->166(43.4%)	160->166(17.9%)	154->160B(12.3%)
39	315.4	31.71	3.932	0.0019	154->160B(27.4%)	154->159B(14.4%)	154->161B(11.4%)
40	313.6	31.89	3.953	0.0080	160->166(43.8%)	159->166(26.1%)	

Four-coordinate Structure **1**

E(SCF)= -4126.441301 a.u.

G= -4125.991810 a.u. S**2= 6.021 Annihilated= 6.000

Alpha-spin HOMO= -4.0230 LUMO= -1.3976 Gap= 2.6254 eV

Beta-spin HOMO= -3.6137 LUMO= -2.8986 Gap= 0.7151 eV

Fe	-0.035495	-0.391577	-0.617074
S	0.226724	-2.723010	-1.150594
S	-3.468850	2.419126	2.623354
S	-0.637342	0.779518	-2.653112
S	4.158980	1.521959	2.948389
N	-1.479834	-0.961756	0.542613
N	1.494015	0.797285	-0.538985
C	-1.795357	-2.286978	0.710075
C	-1.047317	-3.278968	0.003463
C	-1.271872	-4.642496	0.181166
H	-0.649028	-5.359353	-0.358998
C	-2.282495	-5.088327	1.038358
H	-2.458492	-6.155643	1.176111
C	-3.060191	-4.137101	1.709170
H	-3.865417	-4.464448	2.371097
C	-2.834358	-2.772380	1.549751
H	-3.475689	-2.062535	2.073360
C	-0.661839	-2.942157	-2.754140
H	-0.841785	-4.008601	-2.935612
H	-0.007921	-2.531717	-3.534169
H	-1.606581	-2.386750	-2.736682
C	-2.209371	0.045440	1.288122
H	-1.552878	0.930817	1.385999
H	-2.399839	-0.279563	2.331642
C	-3.513626	0.510516	0.658286
C	-4.190969	1.637921	1.184113
C	-5.365812	2.095026	0.568037
H	-5.896805	2.963020	0.957612
C	-5.873867	1.442898	-0.558492

H	-6.789167	1.813803	-1.024252
C	-5.216379	0.328087	-1.079504
H	-5.610759	-0.187765	-1.956670
C	-4.043897	-0.125129	-0.468219
H	-3.510058	-0.988767	-0.867809
C	-4.550130	3.861460	2.897486
H	-4.543919	4.539106	2.033590
H	-4.121178	4.382089	3.762829
H	-5.576902	3.557199	3.139519
C	1.927565	1.363650	-1.713515
C	1.044884	1.407702	-2.839315
C	1.439477	1.935910	-4.068172
H	0.728820	1.935497	-4.897594
C	2.718394	2.476507	-4.228209
H	3.024879	2.892573	-5.188572
C	3.592197	2.470961	-3.134077
H	4.597335	2.885618	-3.241257
C	3.215966	1.930656	-1.907402
H	3.937259	1.907429	-1.089889
C	-1.473965	2.254001	-1.912009
H	-1.549948	3.043853	-2.668243
H	-0.898297	2.600756	-1.045417
H	-2.472411	1.928470	-1.593081
C	2.313979	0.944560	0.649758
H	1.661314	0.792688	1.528516
H	2.682355	1.987378	0.735941
C	3.496436	-0.006954	0.773515
C	4.430876	0.154137	1.824725
C	5.503054	-0.741906	1.948386
H	6.228368	-0.630111	2.754091
C	5.654683	-1.792007	1.038870
H	6.495954	-2.479217	1.150360
C	3.670914	-1.064670	-0.121391
H	2.948053	-1.179079	-0.930898
C	5.564579	1.395240	4.103750

H	6.524906	1.511048	3.584133
H	5.543077	0.451081	4.663859
H	5.436062	2.228745	4.805651
C	4.738380	-1.957431	0.000351
H	4.850501	-2.775809	-0.712855

Summary of calculated electronic transitions (TD-DFT):

#	nm	1000 cm ⁻¹	eV	f	Assignment (excitations with contrib. greater than 10.0%)
1	2594.9	3.85	0.478	0.0001	154->157B(50.9%) 155->157B(15.1%)
2	2015.4	4.96	0.615	0.0002	154->158B(34.4%) 154->160B(12.9%) 154->157B(12.4%)
3	979.3	10.21	1.266	0.0004	154->164B(16.0%) 154->159B(10.2%)
4	896.9	11.15	1.382	0.0008	154->159B(39.1%) 155->159B(12.3%) 154->158B(11.7%)
5	478.7	20.89	2.590	0.0532	156->157B(84.6%)
6	461.3	21.68	2.688	0.0058	155->157B(66.0%) 154->157B(21.6%)
7	436.9	22.89	2.838	0.0017	155->158B(57.0%) 156->158B(31.9%)
8	424.4	23.56	2.921	0.0031	156->159B(32.6%) 156->158B(24.2%) 155->158B(10.9%)
9	423.4	23.62	2.928	0.0200	156->159B(37.8%) 156->158B(28.1%)
10	414.6	24.12	2.991	0.0030	155->159B(55.9%)
11	394.3	25.36	3.144	0.0179	160->161(33.4%) 156->159B(11.0%)
12	390.0	25.64	3.179	0.0038	159->162(35.2%) 160->162(16.0%)
13	360.5	27.74	3.440	0.0022	156->160B(22.5%) 159->167(12.7%)
14	356.6	28.04	3.477	0.0012	157->164(18.9%) 152->163B(12.4%)
15	355.9	28.10	3.484	0.0001	158->166(25.7%) 153->166B(19.7%)
16	355.1	28.16	3.492	0.0083	
17	350.1	28.56	3.541	0.0232	156->160B(28.7%) 160->161(14.8%)
18	339.7	29.44	3.650	0.0329	155->160B(32.5%) 159->161(11.2%)
19	337.2	29.65	3.677	0.0003	153->157B(92.4%)
20	335.9	29.77	3.691	0.0019	159->161(49.7%) 160->161(16.0%) 159->162(12.3%)
21	335.4	29.81	3.696	0.0017	160->162(62.5%) 159->162(14.7%)
22	324.8	30.79	3.817	0.0007	160->163(70.5%) 159->163(14.4%)
23	321.0	31.15	3.862	0.0003	152->157B(90.0%)
24	319.8	31.27	3.877	0.0607	156->161B(29.7%) 160->164(17.5%)
25	317.2	31.53	3.909	0.0244	160->164(52.4%) 156->161B(15.7%) 159->164(10.3%)
26	314.5	31.80	3.943	0.0035	153->158B(60.8%)
27	313.8	31.87	3.951	0.0182	153->158B(24.4%) 155->161B(22.7%)
28	311.9	32.06	3.975	0.0104	154->160B(16.8%) 156->164B(11.5%) 156->162B(10.7%)

29 309.9 32.27 4.000 0.0008 153->159B(67.5%) 153->158B(11.5%)
30 307.9 32.48 4.027 0.0078 156->162B(20.1%) 154->161B(14.4%) 154->160B(13.1%)
31 306.5 32.63 4.045 0.0012 159->165(40.5%) 160->165(24.8%)
32 305.6 32.72 4.056 0.0068 156->162B(22.6%) 156->164B(13.8%)
33 304.2 32.87 4.076 0.0008 159->163(49.1%)
34 303.7 32.93 4.083 0.0006 157->163(18.9%) 159->163(17.3%) 152->158B(16.4%)
35 301.4 33.18 4.114 0.0004 156->163B(19.3%)
36 300.2 33.32 4.131 0.0009 159->164(39.6%) 159->166(21.9%) 160->166(10.0%)
37 298.9 33.45 4.148 0.0046 158->165(21.5%) 153->165B(12.2%) 153->159B(10.7%)
38 298.7 33.48 4.151 0.0091 156->163B(19.9%)
39 298.1 33.55 4.160 0.0018 152->162(15.7%) 159->167(10.5%)
40 296.4 33.74 4.183 0.0004 159->164(29.5%) 159->166(27.8%) 160->166(22.8%)

References:

1. Bruker AXS Inc., Bruker, APEX2, Madison, Wisconsin, USA, 2012.
2. Bruker AXS Inc., Bruker, SADABS, Madison, Wisconsin, USA, 2003.
3. Sheldrick, G. M. Crystal Structure Refinement with SHELXL. *Acta Cryst. C* **2015**, *C71*, 3-8.
4. Farrugia, L. J. WinGX Program Features. *J. Appl. Cryst.* **1999**, *32*, 837-838.
5. Frisch, M. J.; Trucks, G. W.; Schlegel, H. B.; Scuseria, G. E.; Robb, M. A.; Cheeseman, J. R.; Scalmani, G.; Barone, V.; Mennucci, B.; Petersson, G. A.; Nakatsuji, H.; Caricato, M.; Li, H.; Hratchian, P.; Izmaylov, A. F.; Bloino, J.; Zheng, G.; Sonnenberg, J. L.; M. Hada, M.; Ehara, M.; Toyota, K.; Fukuda, R.; Hasegawa, J.; Ishida, M.; Nakajima, T.; Y. Honda, Y.; Kitao, O.; Nakai, H.; Vreven, T.; Montgomery, Jr. J. A.; Peralta, J. E.; Ogliaro, F.; Bearpark, M.; Heyd, J. J.; Brothers, E.; Kudin, K. N.; Staroverov, V. N.; Kobayashi, R.; Normand, J.; Raghavachari, K.; Rendell, A.; Burant, J. C.; Iyengar, S. S.; Tomasi, J.; Cossi, M.; Rega, N.; Millam, N. J.; Klene, M.; Knox, J. E.; Cross, J. B.; Bakken, V.; Adamo, C.; Jaramillo, J.; Gomperts, R.; Stratmann, R. E.; Yazyev, O.; A. J. Austin, A. J.; Cammi, R.; Pomelli, C.; Ochterski, J. W.; Martin, R. L.; Morokuma, K.; Zakrzewski, V. G.; Voth, G. A.; Salvador, P.; Dannenberg, J. J.; Dapprich, S.; Daniels, A. D.; Farkas, Ö.; Foresman, J. B.; Ortiz, J. V.; Cioslowski, J.; Fox, D. J. *Gaussian 09*, Revision D.01; Gaussian, Inc., Wallingford, CT, 2013.
6. Perdew, J. P.; Burke, K.; Ernzerhof, M. Generalized Gradient Approximation Made Simple. *Phys. Rev. Lett.* **1996**, *77*, 3865-3868.
7. Perdew, J. P.; Burke, K.; Ernzerhof, M. Generalized Gradient Approximation Made Simple. *Phys. Rev. Lett.* **1997**, *78*, 1396.
8. Grimme, S.; Antony, J.; Ehrlich, S.; Krieg, H. A Consistent and Accurate Ab initio Parametrization of Density Functional Dispersion Correction (DFT-D) for the 94 Elements H-Pu. *J. Chem. Phys.* **2010**, *132*, 154104-154118.
9. Becke, A. D. Density-Functional Thermochemistry. III. The Role of Exact Exchange. *J. Chem. Phys.* **1993**, *98*, 5648-5652.
10. Lee, C.; Yang, W.; Parr, R. G. Development of the Colic-Salvetti Correlation-Energy Formula. *Phys. Rev.* **1988**, *B37*, 785-789.
11. Schafer, A.; Huber, C.; Ahlrichs, R. Fully Optimized Contracted Gaussian Basis Sets of Triple Zeta Valence Quality for Atoms Li to Kr. *J. Chem. Phys.* **1994**, *100*, 5829-5835.
12. Mayer, I. On Bond Orders and Valences in the Ab initio Quantum Chemical Theory. *Int. J. Quantum Chem.* **1986**, *29*, 73-84.
13. Gorelsky, S. I.; Basumallick, L.; Vura-Weis, J.; Sarangi, R.; Hedman, B.; Hodgson, K. O.; Fujisawa, K.; Solomon, E. I. Spectroscopic and DFT Investigation of [M{HB(3,5-*i*Pr₂pz)₃}₂(SC₆F₅)₂] (M = Mn, Fe, Co, Ni, Cu, and Zn) Model Complexes: Periodic Trends in Metal-thiolate Bonding. *Inorg. Chem.* **2005**, *44*, 4947-4960.
14. Gorelsky, S. I. AOMix—Software for Electronic Structure Analysis. Version 6.90, Oakville, ON, 2017; <http://www.sg-chem.net>